1 Basics of the Vibration of Strings

As a stringed instrument, the guitar belongs to the subgroup of composite chordophones/lute instruments/crossbar instruments. The strings form frequency-determining oscillators; they radiate their vibration either directly as airborne sound or – after conversion into an electrical signal by the pickups – via the guitar amplifier. Being a mechanical oscillator, the string is briefly fed energy by a plucking action … not a lot of energy but enough to entertain an auditorium even without an amplifier. It would actually be possible to heat up one liter of water to boiling temperature using this plucking energy: to achieve this objective, the guitarist would have to pick the string about 60.000.000 times. That sounds worse than it is – picking the string 5 times per second it would take about 2 years if we assume that no break is taken, and that the heat-insulation is perfect. Old Sisiphus would be happy to "enjoy" such working conditions. Admittedly, approaching the topic of producing art from a mechanistical/ operationistical angle receives ambivalent assessment from the involved research disciplines. Elementartistic schools of though have to put up with being by the gestalt-psychologists that the whole is more than the sum of its parts, after all. It doesn't really help to counter the insight "Hendrixian genius is more than pure superposition of vibrations" with the existentialistic appearing question "yeah well – and where is he now?" … all too different are the doctrines. The following considerations therefore target exclusively vibration mechanics – as a part of the whole … as an essential part of the whole.

Translator's remark: *in this chapter, often the bridge and the nut of the guitar are taken as the points between which the guitar string vibrates. Of course, all basic considerations apply to the fretted string in the same way – the string then vibrates between bridge and fret. This is not always explicitly indicated, and therefore the term "nut" should be considered to appropriately include the term "or fret", as well.*

1.1 Transversal waves

The strings of an electric guitar are made of steel, with its **density** ρ just below $8 \cdot 10^3\ \mathrm{kg/m^3}$. A steel string with a **diameter** D is stretched to the **length** L by applying the **tension force** Ψ. Fretting the string on the fretboard shortens the length. Typical lengths are just shy of 65cm for the open (unfretted) string (= scale M). Plucking the string (with a finger or a pick) displaces the string in the transversal direction; subsequently there is a free, damped vibration. After the plucking-release, a transversal motion (transversal wave) propagates from the plucking position in both directions of the string. The **propagation speed** c of this wave running along the string is (with $\rho = 8 \cdot 10^3\ \mathrm{kg/m^3}$):

$$c = \frac{2}{D}\sqrt{\frac{\Psi}{\pi\rho}} = \frac{\sqrt{\Psi/\mathrm{N}}}{D/\mathrm{mm}} \cdot 12{,}6\,\frac{\mathrm{m}}{\mathrm{s}}$$

Propagation speed

Given a string of a diameter of 0,35 mm and a tension force of 50 N, c calculates to 255 m/s. However, this propagation speed (in the direction of the string) must not be confused with the velocity that the string oscillates back and forth with in the transverse direction. To avoid any confusion, the transverse velocity is termed **particle velocity** v. More detailed investigations reveal that c is not constant but depends on the frequency (dispersion); more about this in Chapter 1.3.

Moving with the propagation speed, the transversal wave runs off in both directions and is reflected at both ends (nut and bridge, respectively). As a reflection, it then returns to the point of origin. We may imagine and model the process of reflection as a superimposed signal originating from a **mirror source** positioned behind the end of the string (**Fig. 1.1**). In this model, the primary wave excited by the plucking runs beyond the end of the string (i.e. it is not reflected), but an additional superimposed (added) mirror wave runs opposed to the primary wave. At the fixed end of the string, both waves meet. It is obvious that the displacement of the mirror wave needs to be in **opposite phase** to the primary wave such that the end of the string indeed remains (ideally) at rest and immobile. This phase reversal is valid at both nut and bridge in the same way.

Fig. 1.1: Propagation of a transversal wave on a clamped string.

As the reflections arriving from nut and bridge reach the origin-point of the plucking, they continue further, are then reflected again at the respective other end of the string, and run back to the plucking point with the original phase. Arriving there after having covered $2L$, one full **period of the fundamental oscillation** T has passed. The reciprocal of T is the **fundamental frequency** f_G of the string. A steel string of a length of 0,65 m and a diameter of 0,35 mm oscillates – at a tension force of 50 N – with a fundamental frequency of 196 Hz (note G_3).

The frequencies of the open strings (in regular tuning) are **E** = E_2 = 82.4Hz, **A** = A_2 = 110Hz, **d** = D_3 = 146.8Hz, **g** = G_3 = 196Hz, **b** = B_3 = 246.9Hz, and **e'** = E_4 = 329.6Hz.

The fundamental frequency of the string depends on the **tension force** Ψ, the **density** ρ, the **diameter** D, and the **length** L. Quadrupling the force, or halving the length, or halving the diameter, respectively, doubles the fundamental frequency:

$$f_G = \frac{c}{2L} = \frac{\sqrt{\Psi / \pi\rho}}{DL} = \frac{\sqrt{\Psi / \mathrm{N}}}{D/\mathrm{mm} \cdot L/\mathrm{m}} \cdot 6{,}3\,\mathrm{Hz}$$ Fundamental frequency

The tension force Ψ required to obtain a certain fundamental frequency calculates based on the length L of the string, and on the material data of the density ρ and the diameter D. Fundamental frequency and string-length appear as a product; given a string tensioned with a constant force, fundamental frequency and string length are therefore reciprocal to each other:

$$\Psi = (f_G \cdot L)^2 \cdot \pi\rho D^2 = c^2 \cdot \pi\rho D^2 / 4$$ Tension force

Because the actual oscillation processes are rather complicated, idealizing models are employed. In the simplest case, planar polarization, frequency-independent propagation speed, absence of losses, and ideal reflections are assumed. The string is described as a linear, time-independent LTI-system.

The periodic repetition caused by the reflections can be seen as a (temporal) convolution of the excitation impulse with a causal Dirac-pulse. Causal means that the signal is zero for the negative time axis. A causal Dirac-pulse contains equidistant Dirac-impulses for $t \geq 0$. A temporal convolution corresponds, in the spectral domain, to a multiplication of the excitation spectrum with the spectrum of the causal Dirac-pulse. This latter spectrum necessarily is complex, since the time-function (causal Dirac-pulse) is neither odd nor even (mapping theorem). Using partial fraction decomposition, it can be shown that a co-tangent-shaped spectrum of the imaginary part is linked to the causal Dirac-pulse; the spectrum of the real part is a spectral Dirac-comb. This complex spectrum would have to be multiplied by the excitation spectrum – however this is still too complicated for most considerations.

For this reason, further idealization is in order. The (un-damped) oscillation is not induced at $t = 0$ but continues from the infinite past to the infinite future. The period of the oscillation may be developed into a Fourier series since it is in a steady state with regard to its periodicity. A **line spectrum** results as the spectrum of the oscillation, with the frequency lines at the integer multiples of the fundamental frequency.

This way, the overall oscillation can be seen as the sum of superimposed (added) single tones – they are called partials or (because of the integer frequency relations) **harmonics**. The fundamental is the 1st harmonic, with the 2nd harmonic located at double the frequency of the fundamental. In music, the 2nd harmonic is called the 1st **overtone**. This terminology extends to the higher harmonics correspondingly (3rd harmonic = 2nd overtone, etc.).

Reality differs considerably from these idealizations. A line spectrum requires a periodic signal of infinitely long duration. In signal theory, the term 'periodic' implies that a certain section of the signal is infinitely repeated in identical shape. However, as it oscillates back and forth, the string looses energy, and therefore an identical repetition of any signal section is not possible. The oscillation of the string therefore is a non-periodic signal that has no actual line spectrum affiliated to it; rather, the spectral lines are broadened into funnels due to the damping. The reasons for the energy loss are **dissipation** and radiation: the motion energy in the string is partially converted directly into heat, and partly radiated as sound-energy. The frequency dependent propagation speed (**dispersion**) – discussed more extensively in Chapter 1.3 – constitutes an additional effect that must not be ignored for more detailed investigations.

Even though the string oscillation is in fact of dispersive and dissipative character, it is still purposeful for the understanding of the motion processes to use a simplified, idealized view. This holds in particular as long as we only regard short sections of the time signal.

An idealized plucking will displace the string triangularly (**Fig. 1.2**). After the pick (or the finger) has lost contact to the string, the latter will ideally oscillate freely and without damping. The shape of the lateral displacement can be seen as superposition of two partial waves running in opposite directions. Both partial waves are identical at the moment of plucking but run away from each other in opposite directions for $t > 0$; the magnitudes of both propagation velocities are equal. For $t = 0$, the displacement of each partial wave at the nut and the bridge is zero; it is at its maximum value at the plucking location. The triangular shape continues in a point-symmetrical (odd) manner at the nut and the bridge as mirror wave. The displacements of both *partial waves* are superimposed to yield the displacement of the string. The same holds correspondingly for all derivatives, e.g. for the propagation speed.

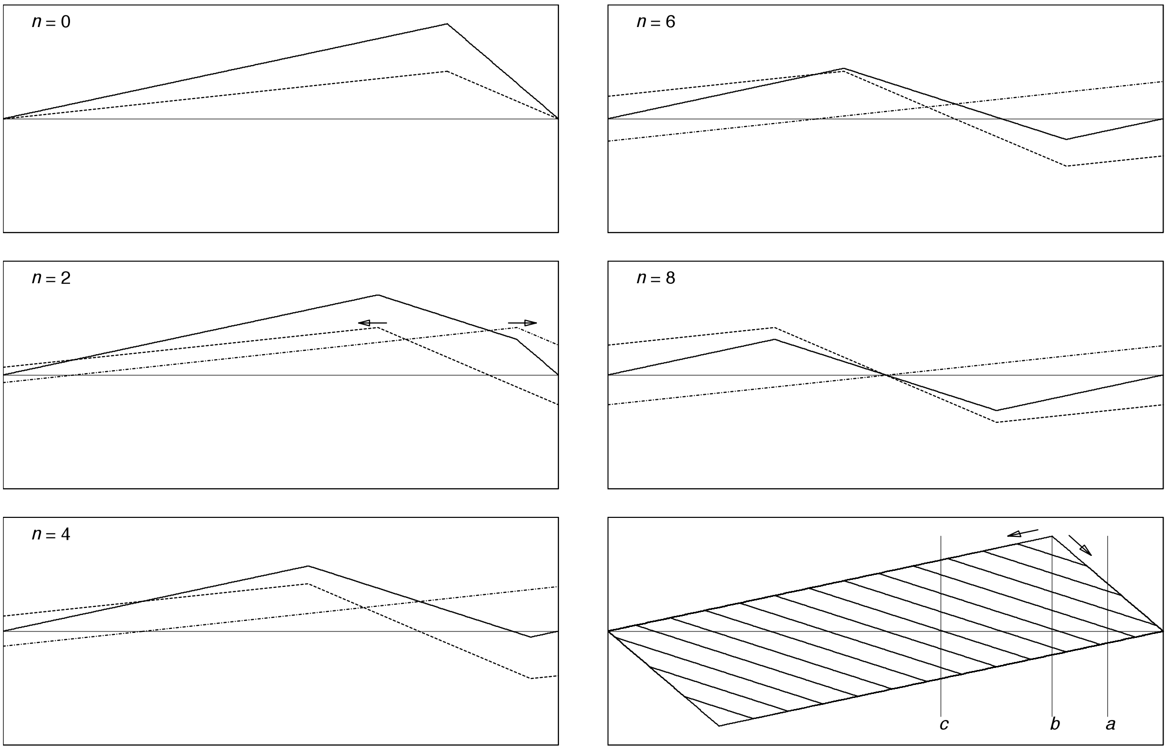

Fig. 1.2: Propagation of a triangular wave after plucking the string. The phase shift is $\varphi = n \cdot \pi / 16$.
The string (indicated as the bold line) is modeled as superposition of two partial waves running away from each other. The abscissa is the coordinate along the string (length of the string); the ordinate is the lateral displacement. A parallelogram yields the delimitation line for the string displacement (lower right). These diagrams are not time functions!

The actual string vibration is the sum of **two partial** waves running in opposite directions. Both triangularly displaced partial waves run at constant speed. The particle velocity of each point on the string is constant per section; however, the movement in one direction happens with a different particle velocity compared to the movement in the other direction. Superimposing both waves yields an unexpected result: each location on the string is either at rest, or it vibrates with the constant (!) **particle velocity** $\pm v$. String locations close to the nut or to the bridge do not vibrate more slowly but during a shorter time compared to locations at the middle of the string (**Fig. 1.3**).

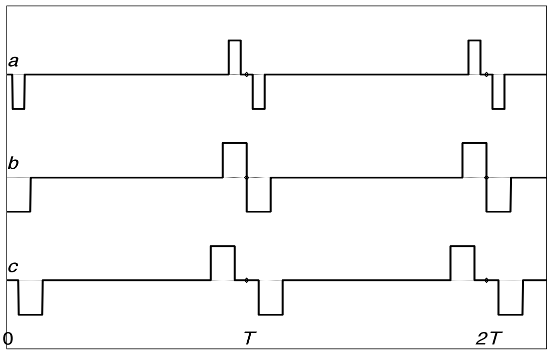

Fig. 1.3: Time function of the particle velocity of the string at three different points a, b, c (see Fig. 1.2 for comparison). From this, the time function of the displacement of these points can be derived via integration. For the v-spectrum, the superposition of two line spectra with phase-shifted si-envelope results. A temporal integration corresponds to a division by $j\omega$ in the frequency domain.

In this model-consideration it is important to distinguish the actual string oscillation (measurable in reality), and the components from which it is put together in the model. The partial waves may not be considered in isolation; they are "artificially generated" to support the visualization of the concept.

1.2 Wound strings

The thinner strings of the electric guitar (E_4, B_3) consist of solid steel. If the thicker (bass-) strings (E_2, A_2, D_3, sometimes G_3 as well) were manufactured the same way, unavoidable flexural stiffness would result in considerable inharmonicities (Chapter 1.3). For this reason, a thin core made of steel is wound with a helically abutting winding (**Fig. 1.4**). For electric guitars, the winding consists of steel or nickel, while for acoustic guitars it is made of bronze. Using this construction, the flexural stiffness is determined mainly by the core. The winding merely contributes the required additional mass.

Several criteria are relevant for the relationship $\boldsymbol{\kappa = D_K/D_A}$ between core diameter D_K and the outer diameter D_A: in order to reduce the flexural stiffness, κ should be made as small as possible. However, the normal stress now very quickly approaches the limit of tensile strength even for high-strength steel. Simple machinery steel, for example, has a **minimum tensile strength** of around 430 N/mm^2 (St 44). For strings, this would be not adequate at all since – for regular tuning and in rest condition – up to 2000 N/mm^2 is required here. During playing, additional strain occurs that (in the interest of long durability) still needs to remain well below the breaking point. Moreover, high endurance towards changing strain is demanded as well. In addition, the string must not corrode too fast, it should not be too brittle (in order to agree with string bending), and it moreover needs to have certain magnetic properties. Overall, these are very challenging demands – not easily fulfilled by just any manufacturer of wires.

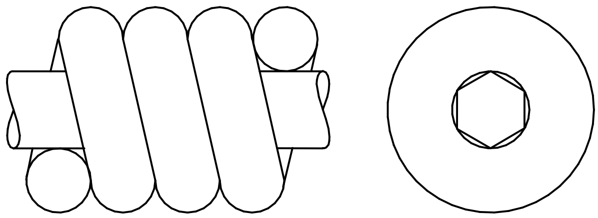

Fig. 1.4: Wound string.
The string-core is either round or polygonal (e.g. hexagonal).

For most wound strings, the **core-diameter** measures 1/3rd to 2/3rd of the outer diameter. In particular for the higher-frequency strings, a smaller κ-value leads to breakage, and moreover the winding-wire would have to be bent very strongly. Higher κ-values relieve the core but bring stronger inharmonicities, and also result in too small a diameter of the winding wire (this also calling for issues with durability). Besides the ratio of core diameter to overall diameter, the absolute values are significant, too. To generate a certain pitch (e.g. E_2), the heavier strings need to be (and may be) stretched more than the light strings. Doubling the diameter quadruples the mass; if the pitch is supposed to remain constant, the tension force also needs to be quadrupled – with the normal tension (pulling force / cross-sectional area) remaining unaffected by this.

The winding of a string often employs round wire; **flat wire** is used more rarely. Due to the oblique grooves, strings wound with round wire feel somewhat rough; strings wound with flat wire (flatwound strings) give a feel similar to the plain strings but they sound differently. Somewhere midway we find sanded-down strings: here the core is first wound with round wire, and subsequently the outer sections of the winding are slightly sanded in order to reduce the surface roughness.

 Translation by Tilmann Zwicker

On acoustic guitars, heavy strings facilitate a louder sound but require to be pressed down onto the fretboard with more force. The signals generated by electric guitars can be amplified to almost any degree, and therefore we frequently find, on these instruments, lighter strings than on acoustic guitars. In fact, it was only the reduction of the tension- and thus playing-forces by up to 50% that enabled the development of new techniques (bending strings, finger vibrato) on the electric guitar.

Every string manufacturer offers sets of strings with different diameters – designations are usually "heavy", "medium", "light", or "super light". For a more precise characterization, all string diameters are in addition given in mil (1 mil = 1/1000 inch = 25.4 mm /1000). On electric guitars, the so-called 009-set is found quite often, consisting e.g. of strings with the diameters 9-11-15-24-32-42. However, there are 009-sets also with different gradation, for example 9-11-16-26-36-46. In string sets with thinner strings (“light gauge strings”), the three treble strings are solid (“plain”) while the heavier strings are wound; in heavier gauge string sets, the G-string is would, as well.

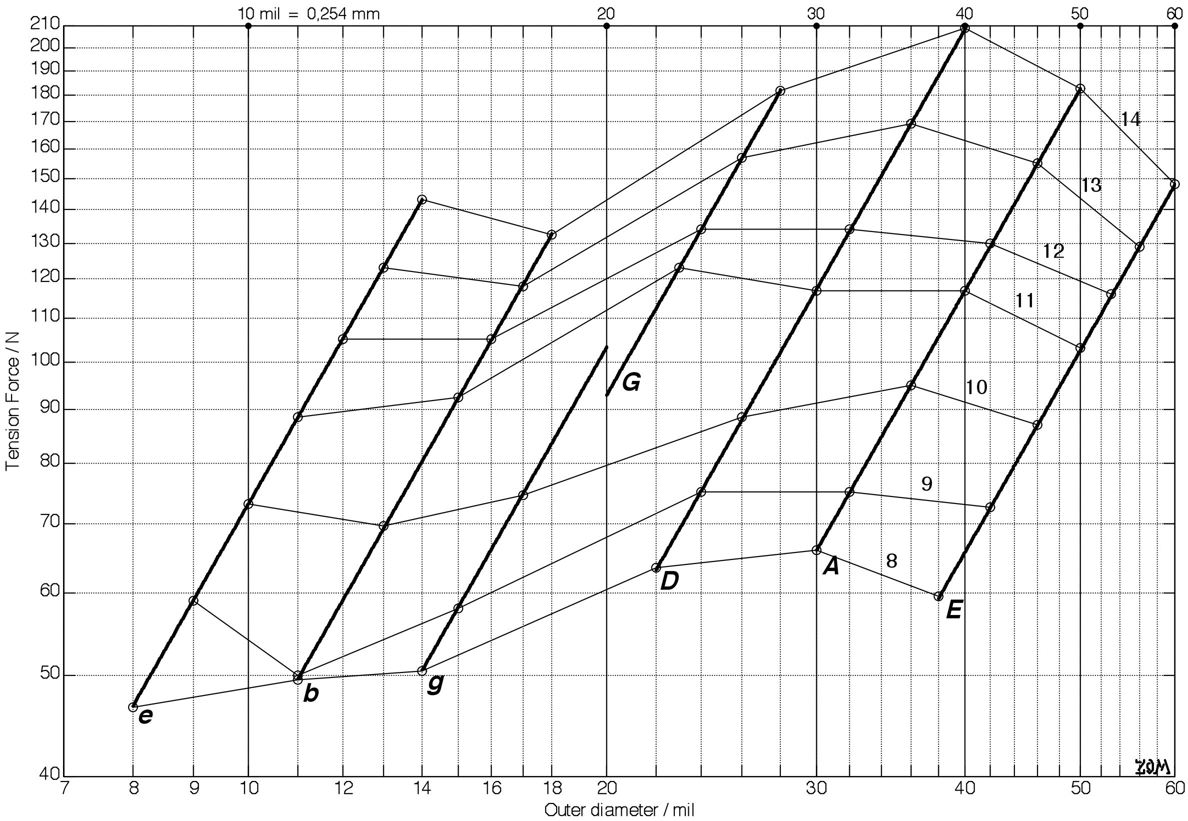

Fig. 1.5: Tension-force of a string dependent on the outer diameter. ρ_{core} = 7900 kg/m^3, $\rho_{winding.}$ = 8800 kg/m^3. For the string length, 25.5" = 64.8cm (e.g. Stratocaster) was taken; shorter lengths decrease the tension force Ψ. The effect of κ on Ψ is small. 013- and 014-string-sets are mainly found on steel-string acoustic guitars.

Fig. 1.5 shows how tension force Ψ and string diameter are related. The strings are depicted as steeply inclined lines, with the G-string shown both with and without winding. Frequently used diameter combinations are shown as a shallow curved line. The calculations are based on rigid (unyielding) string-bearings. Spring-loaded bearing (e.g. a vibrato system) necessitates higher tension forces. For frequency dependent spring effect see Chapter 2.5.2.

For solid strings, the **tension force of the string** Ψ is calculated from the density ρ, the fundamental frequency f_G, the (outer) diameter D, and the string length (scale) M:

$$\Psi = \pi \cdot \rho \cdot \left(f_G \cdot D \cdot M\right)^2$$ Tension force of the string

Due to the air enclosed in the winding, the **density** of **wound strings** is about 10% less compared to solid strings (given the same outer diameter):

$$\overline{\rho} = \rho_{wound} = \left[\kappa^2 + \left(1-\kappa^2\right)\cdot\frac{\pi\cdot\rho_W}{4\cdot\rho_K}\right]\cdot\rho_{plain} \approx 0.9\cdot\rho_{plain}; \qquad \kappa = D_{\mathrm{K}}/D_{\mathrm{A}}$$

In this formula, ρ_W is the density of the winding, ρ_K is the density of the core material. ρ_{plain} indicates the density of a solid string of the same outer diameter (used for comparison), $\overline{\rho}$ is the average density of the wound string. $\kappa = D_{\mathrm{K}}/D_{\mathrm{A}}$ = core- / outer-diameter. A more precise consideration requires minor corrections in case the core is not round but features a square or a hexagonal cross-section, and if the winding comprises sanded down round wire, or flat wire.

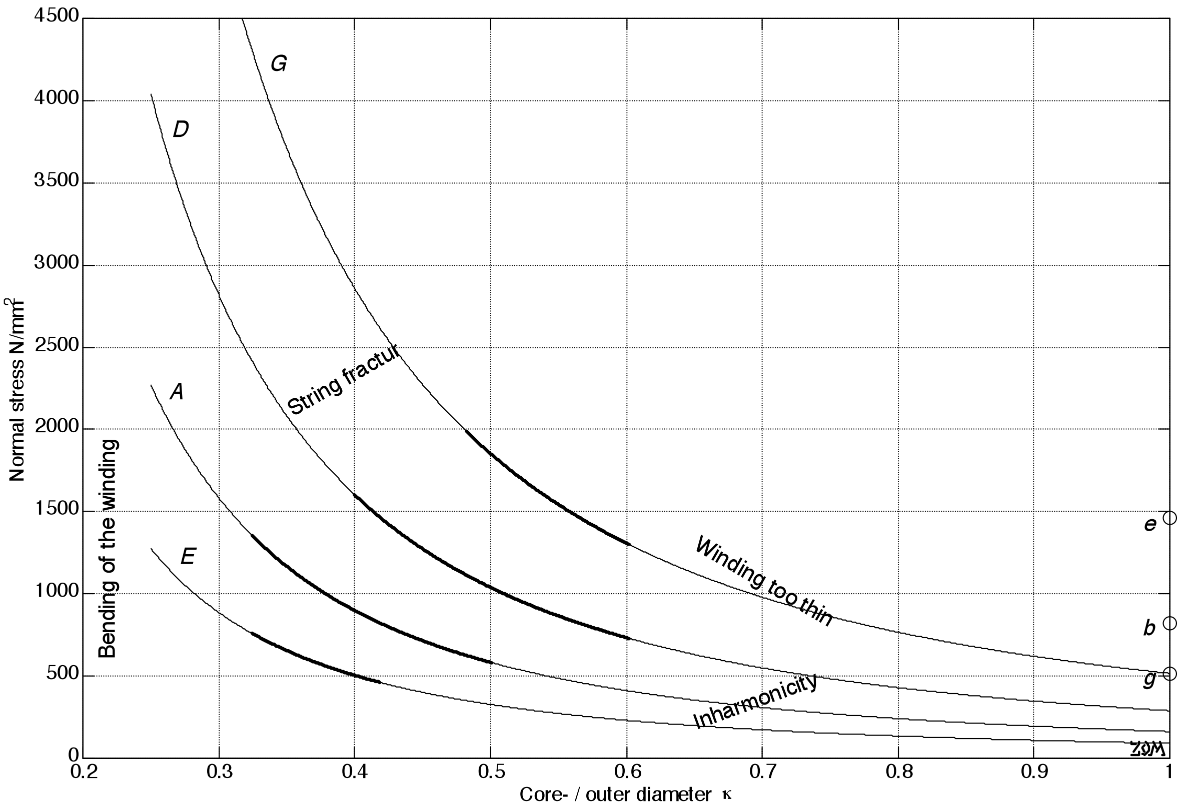

Fig. 1.6: Normal stress of the string dependent on κ. Customary values are shown in bold. The values for the (solid) e-, b- und g-strings are marked as a circle at the right border of the graph. M = 25.5" = 64.8 cm . The representations are valid for stiff (unyielding) string bearings; spring-loaded bearings (vibrato) yield increased normal tension.

 Translation by Tilmann Zwicker

For solid strings, the **normal tension** σ (tension force / cross-sectional) calculates as:

$$\sigma = \frac{4\Psi}{\pi D^2} = 4\rho \cdot (f_G \cdot M)^2$$ Normal tension (solid string)

Given equal fundamental frequency and length, the normal tension does not depend on the string diameter. If light strings seem to break more easily than heavy ones, this is due to the additionally acting plucking force – light strings offer little overhead here. For wound strings, σ calculates as:

$$\sigma = \frac{4\Psi}{\pi D_\mathrm{K}^2} = \frac{4\overline{\rho} \cdot (f_G \cdot M)^2}{\kappa^2}$$ Normal tension (wound string)

An average density $\overline{\rho}$ reduced by 10% needs to be applied as density for wound strings. A particular influence is due to the ratio of the diameters κ. **Fig. 1.6** shows, for all 6 strings, the normal tensions; towards the top, the risk of breaking the string increases; towards the right, there is more inharmonicity (Fig. 1.7). Contrary to fracture of the string (which of course must be avoided), inharmonicity is not inherently a bad thing – it even may impart a special "liveliness" to the sound of the string (Chapter 8.2.5).

The **inharmonicity** that appears in particular for heavy strings in their higher partials is due to the flexural stiffness. According to [1], the frequency of the n-th partial calculates as:

$$\boxed{f_i[n] = n \cdot f_G \cdot \sqrt{1 + bn^2}} \qquad b = \left(\frac{\pi D}{8M^2 f_G}\right)^2 \cdot \frac{E}{\rho}$$ Spreading of partials

This formula (dating back to Lord Rayleigh) holds for solid strings with D as the string diameter. For wound strings we rearrange the math as follows:

$$b = \frac{\pi^2 B}{4M^4 f_G^2\, m'} \qquad B = \frac{E\pi D_\mathrm{K}^4}{64} \qquad m' = \frac{\pi D_\mathrm{A}^2}{4}\overline{\rho}$$

Here, B is the flexural stiffness that depends on the core diameter D_K and on Young's modulus E, and m' is the **length-specific mass** depending on the outer diameter D_A. We obtain as the parameter of inharmonicity b:

$$b = \frac{\pi^2 E}{64 M^4 f_G^2\, \overline{\rho}} \cdot \kappa^4 D_\mathrm{A}^2$$ Inharmonicity-parameter

In **Fig. 1.7**, several ranges are marked for b. These encompass, for wound strings, the range of customary outer diameters, and of customary values of κ (compare Fig. 1.6). For solid strings (lower-case letters), $\kappa = 1$ holds.

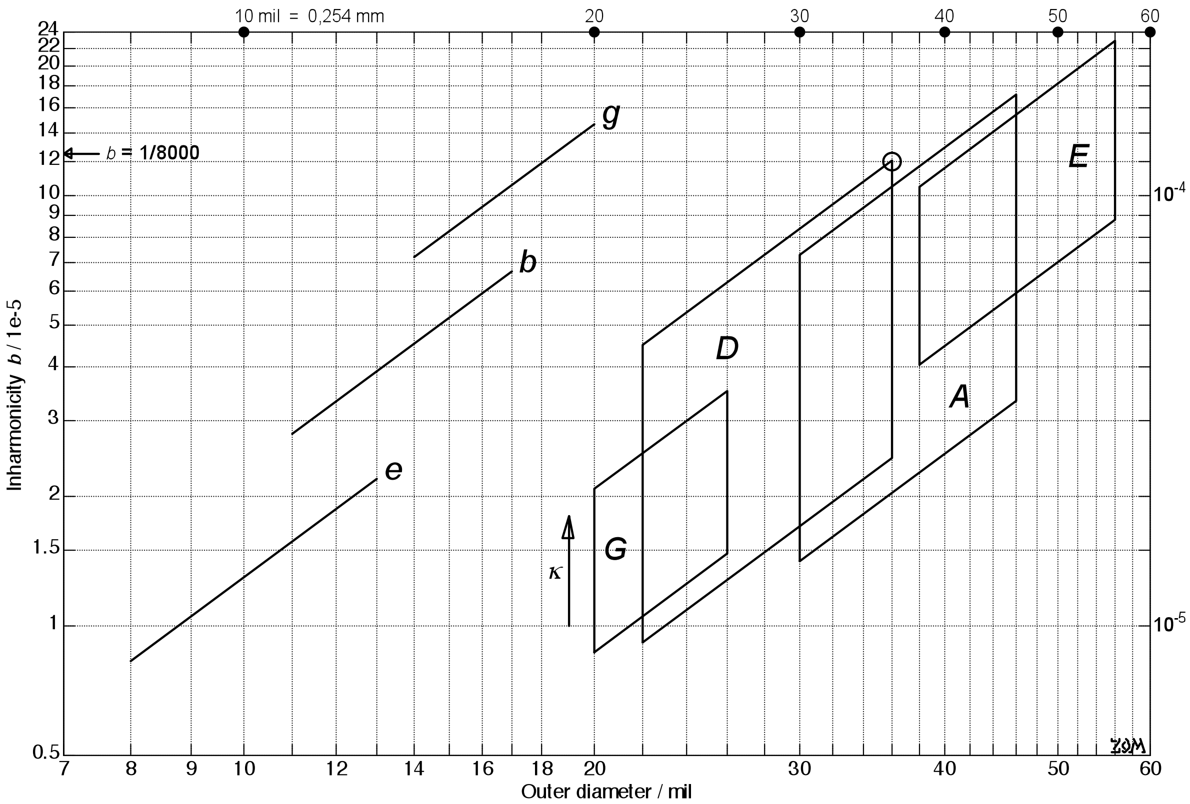

Fig. 1.7: Parameter b for the inharmonicity of partials of typical guitar strings; *E-A-D-G* = wound, *g-b-e* = plain. For a wound D-string with an outer diameter of 36 mil, we obtain: b = 12e-5 for $\kappa = 0.6$; Core-/outer-diameter: κ_E = 0,33 – 0,42 κ_A = 0,33 – 0,50 κ_D = 0,40 – 0,60 κ_G = 0,48 – 0,60. Scale = 65 cm. For a scale of 63 cm, all values for b need to be increased by 13%.

Material	Density ρ in 10^3 kg / m^3	Young's modulus E in 10^9 N / m^2
Steel	7,8 - 8,1	200 - 220
Nickel (Ni)	8,90	199
Copper (Cu)	8,92	120
Brass (Cu, Zn)	8,1 - 8,6	≈ 100
Bronze (Cu, Sn)	8,2 - 8,9	≈ 110
German silver (Cu, Zn, Ni)	≈ 8,6	≈ 130
Nylon (Polyamid)	≈ 1,2	≈ 3,5

Table: Material-data. Steel, Brass, Bronze and German silver are available in various compositions.

1.3 Inharmonic partials

The simple ideal string has a length-specific mass m', and a tension-stiffness $\pi^2 \Psi/L$ created by the tension force Ψ. Conversely, the real string also includes a flexural stiffness that impedes bending the string – this is an undesirable effect that causes **dispersive wave propagation**. The heavier the string is, and the less it is tensioned, the more the flexural stiffness manifests itself (i.e. especially in the bass strings of the guitar). To achieve an improvement, heavy strings are wound with thin wire of one or more layers. The flexural stiffness is then predominantly determined by the thinner core, while a high mass loading is still possible. However, since the core cannot be made arbitrarily thin, the impact of dispersion may only be reduced but cannot be removed. Precise analyses indicate a propagation speed $c(f)$ that increases towards higher frequencies. It causes the partials to "spread out" and loose their harmonicity to a certain degree. Therefore, the term "harmonics" is incorrect in the strict sense of the word and may be replaced by the term "partial".

1.3.1 Dispersion in the frequency domain

In a linear (or at least linearized) system, any oscillation shape may be represented as a superposition of single mono-frequent oscillations. The propagation of a transversal wave is described by the **wave equation**. A position- and time-dependent transverse displacement $\underline{\xi}(z,t)$ is created along the propagation direction z, with the temporal derivative being the particle velocity.

$$\underline{\xi}(z,t) = \hat{\xi} \cdot e^{j\varphi_0} \cdot e^{j\omega t} \cdot e^{-jkz}$$ Wave equation

In this equation, $\hat{\xi}$ represents the oscillation amplitude, φ_0 indicates the phase angle at the position $z = 0$ and at the point in time of $t = 0$, ω is the angular frequency, and k is the wave number. The angular frequency yields the periodicity in time $T = 2\pi/\omega$; the wave number yields the periodicity in space $\lambda = 2\pi/k$. For a fixed position z, the phase grows linearly with the time t, for a fixed point in time, the phase decreases linearly with the position z:

$$\varphi(z,t) = \varphi_0 + \omega t - kz$$ Phase function

The periodicity in space (wave length λ) and the periodicity in time (oscillation period T) are linked via the propagation speed (= phase speed) c:

$$c = \omega/k = \lambda/T$$ Propagation speed

A steady free oscillation can only originate if all reflections running in a z-direction superimpose with the same phase, i.e. if the phase shift across the length $2L$ amounts to an integer multiple of 2π:

$$\left.\Delta\varphi = n \cdot 2\pi = k \cdot 2L \quad \right\} \qquad f_n = \frac{n \cdot c}{2L} = n \cdot f_G$$ Frequencies of partials

In this equation, the propagation speed c is assumed to be frequency-*in*dependent; the partials f_n are then situated at integer multiples of the fundamental frequency.

However, in reality the string features **dispersive wave propagation** (i.e. the propagation speed is frequency dependent): high-frequency signal run at higher speeds than low-frequency signals, and therefore frequencies of the partials grow progressively (i.e. are spread out) with increasing frequency. The underlying mechanism is the already mentioned flexural stiffness that manifests itself in particular in oscillation shapes with strong curvature (i.e. at small wave-lengths = at high frequencies). It should be noted that this is a linear effect. The frequencies of the **inharmonically** spread out partials can be calculated with the following formula [appendix]:

$$f_i = n f_G \sqrt{1 + b n^2} \qquad \text{with} \qquad b = \left(\frac{\pi \kappa^2 D_A}{8 L^2 f_G} \right)^2 \cdot \frac{E}{\rho} \qquad \text{Spreading of partials}$$

Herein, the symbols mean: f_i = frequency of inharmonic partial, f_G = fundamental frequency without dispersion, n = order of the respective partial, b = parameter of inharmonicity, E = Young's modulus (approx. $2 \cdot 10^{11}$ N/m^2), D_A = outer diameter, κ = core- / outer-diameter, L = length of the string, ρ = density.

With a **solid** string of a diameter of 1,2 mm tensioned such that a fundamental frequency of 82,4 Hz results, the dispersion would detune the 20th partial from 1648 Hz to 2774 Hz – quite a considerable effect. Using, instead of a solid string, a **wound** string of the same length-specific mass, the flexural stiffness is reduced – and so is the inharmonicity. In wound guitar strings, the core diameter is smaller than the outer diameter by a factor of about 0.3 to 0.6. The density ρ will be about 7900 kg/m^3 for solid strings, while for wound strings the effective density $\overline{\rho}$ is about 10% less than the core density (Chapter 1.2). Given a wound E_2-string (with an outer diameter of 1,3 mm), the calculation yields (using b = 1/8141) a spreading of the 20th partial from 1648 Hz to 1688 Hz, i.e. by 2,5%.

In the formula of the spreading-parameter b, the length of the string L occurs with the power of 4, while the fundamental frequency only occurs with the power of 2. If, for example, fretting the octave halves the string-length, the percentile in detuning of the 20th partial increases from 2,5% to 9,5% – that is from just shy of a half-step to three half-steps. However: the 20th partial of the fretted octave lies in a different frequency range, and the direct comparison between the 20th partial of the open string and the 10th partial of the octave shows the same detuning of (2,5%). In other words: for a given string and the same absolute frequency, the inharmonicity is always of the same strength irrespective of the fretted note.

The **down-tuning** of a guitar also increases the inharmonicity: if – in the above example – the low E-string is down-tuned by a whole step (82.4 → 73.4 Hz) and the regular-tuned open E-string is compared with the down-tuned E-string fretted at the 2nd fret (i.e. in both cases we have the note E_2), the inharmonicity of the 20th partial is at 2.5% for the regular tuning, and 3.9% for the down-tuning.

At this point we shall not investigate how far these inharmonicities of the partials are actually audible; details about the topic are included in Chapter 8.2.5. [10] reports about hearing experiments, and in [2] a computation method for piano strings is developed.

Fig. 1.8 shows the relationship between the order n of the partial and the spread frequency f_i as it can be observed for a wound low E-string of a diameter of 1,3 mm. The fundamental frequency is 82,4 Hz, the spreading parameter is b = 1/8000.

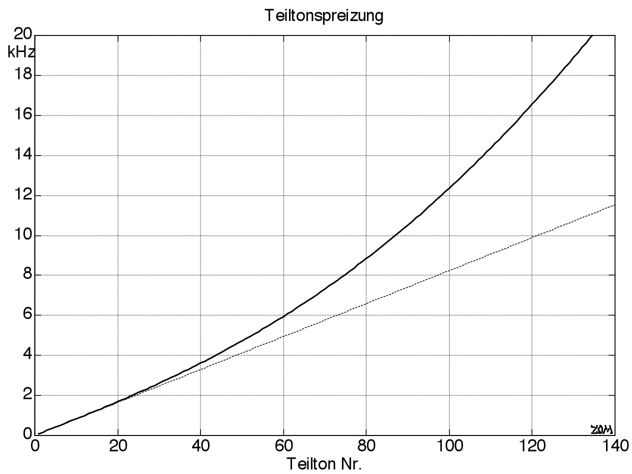

$$f_n = n \cdot f_G$$

$$f_i = n \cdot f_G \sqrt{1 + bn^2} = f_n \sqrt{1 + bn^2}$$

$$f_n = f_G \sqrt{\frac{\sqrt{1 + 4b(f_i / f_G)^2} - 1}{2b}}$$

Fig. 1.8: Inharmonic spreading of the partials for a low E-string. The thin line marks a harmonic relation. "Teiltonspreizung" = spreading of the partials; "Teilton Nr." = partial no.

Fig. 1.8 attributes to a given partial its spread-out frequency. For the following considerations, however, the reverse relationship is required, as well: we have a partial at a given frequency f_i, and want to know how much was it spread, or what its frequency f_n is. **Fig. 19** provides the answer. The abscissa f_i shown corresponds to the ordinate in Fig. 18.

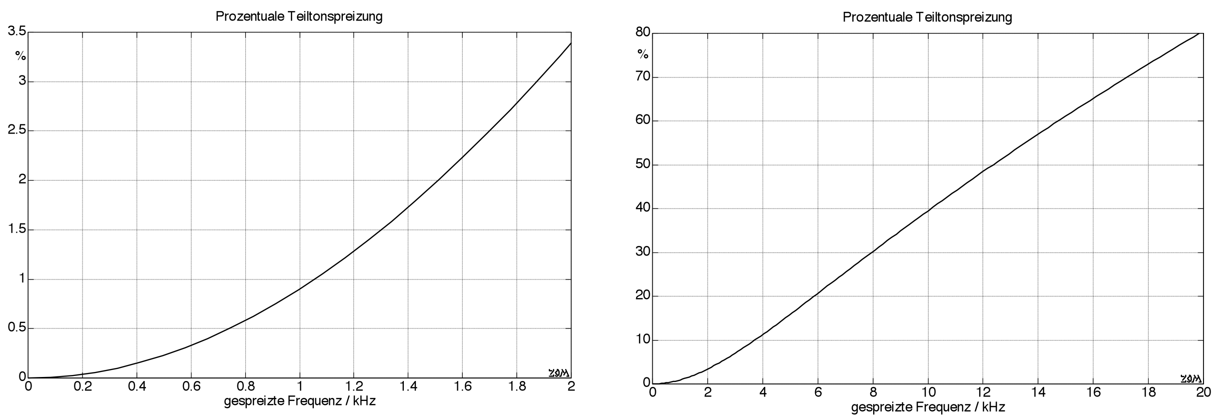

Fig. 1.9: Spreading (on a percentage basis) of partials as a function of the (spread-out) frequency (low E-string), b = 1/8000. "Prozentuale Teiltonspreizung" = spreading of partials on a percentage basis; "gespreizte Frequenz" = spread frequency.

Only at the discrete frequencies $f_i[n]$ with n = *integer* we find an in-phase superposition of all waves running in the same direction. For a full revolution ($z = 2L$), the phase shift amounts to $n \cdot 2\pi$, and the travel time required corresponds to the n-fold period T of the oscillation, i.e. $\tau_p = n / f_i$. Because here the travel time for a specific phase is referred to (e.g. for the zero crossing), the term used is the **phase delay** τ_p, with the corresponding propagation speed being the **phase speed** c_p.

$$\tau_p = \frac{n}{f_i} = \frac{1}{f_G \sqrt{1 + bn^2}} \qquad \text{for } z = 2L; \qquad c_p = \frac{2L}{\tau_p} = 2Lf_G \sqrt{1 + bn^2}$$

When using the formulas giving phase delay and phase speed, we need to bear in mind that the spread-out frequency is used. It is for this reason that the right-hand side of the equation should contain f_i but not f_n:

$$\tau_p(2L) = \frac{\sqrt{2}}{f_G\sqrt{1+\sqrt{1+4b\cdot(f_i/f_G)^2}}}; \qquad c_p = \sqrt{2}\cdot L\cdot f_G\cdot\sqrt{1+\sqrt{1+4b\cdot(f_i/f_G)^2}}$$

Fig. 1.10 depicts the frequency dependency of the phase delay and the phase speed. On the abscissa we find the spread frequency f_i, i.e. the frequency where the oscillation actually occurs. The calculation here is done for the low E-string (E_2) with b = 1/8000.

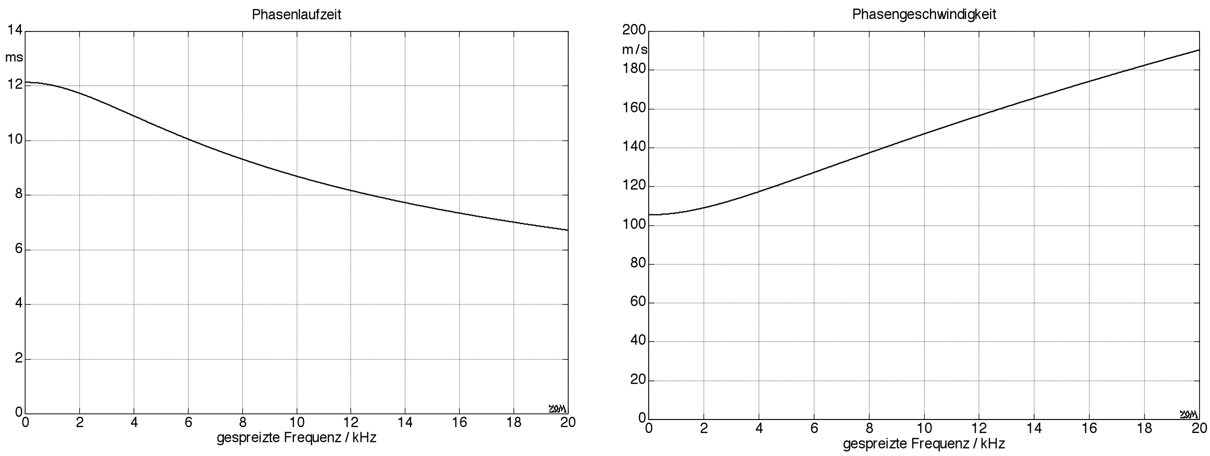

Fig. 1.10: Phase delay ("Phasenlaufzeit") (z = $2L$) and phase speed ("Phasengeschwindigkeit"), low E-string, b = 1/8000. "gespreizte Frequenz" = spread-out frequency

For the following considerations, theoretical calculations are compared to measurements. An **Ovation guitar** (Viper EA-68) constitutes the measuring object – it includes a piezo-pickup mounted in the bridge. The Viper is not a typical Ovation: its body has a thickness of 5 cm, and being largely solid it can be counted as a solid-body guitar. The built-in amplifier was not used; rather, the pickup was directly connected to an external measuring amplifier featuring very high input impedance. For the majority of the measurements, D'Addario Phosphor-Bronze strings EJ26 were deployed (.011 – .052). If not specified otherwise, the guitar was in standard tuning E-A-D-G-B-E.

Fig. 1.11 juxtaposes calculation and measurement. There is a problem in principle with the (or any) spectral analysis: to obtain a high frequency resolution, a measurement with a long time duration is necessary – analysis-bandwidth and -duration are reciprocal, after all. However, with long measurement duration, dissipation makes itself felt at high frequencies – the signal is not in steady-state anymore. Any measurement will therefore represent a compromise. In Fig. 1.11, the duration of the analysis amounts to 85 ms, and instead of narrow spectral lines the result are funnel-shaped extensions (DFT-leakage). Pointing upwards, the tips of the funnels indicate the frequency of the respective partial; the minima of the curves are of no significance. To compare, Fig. 1.11a holds (as dots) the calculation results for *harmonic* partials: the correspondence is weak – at 2,3 kHz, the frequency-discrepancy is already as big as the distance between two partials. Fig. 1.11.b shows the *spread* partial frequencies with a significantly better correspondence. Any remaining differences will be discussed later – as will be the frequency-dependence of the level.

 Translation by Tilmann Zwicker

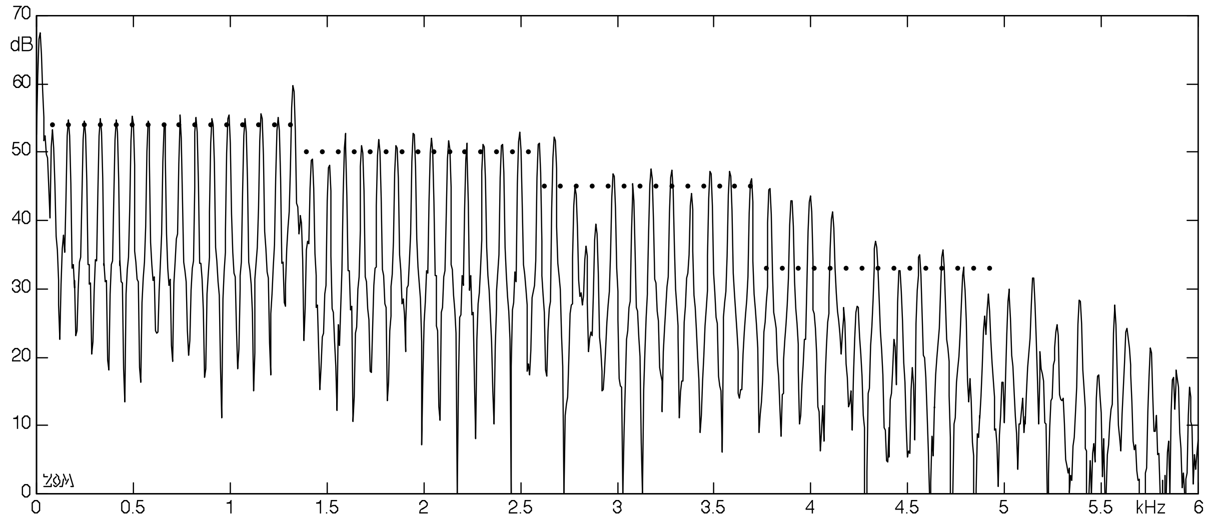

Fig. 1.11.a: Measured spectrum (lines), calculated *harmonic* partials (dots).

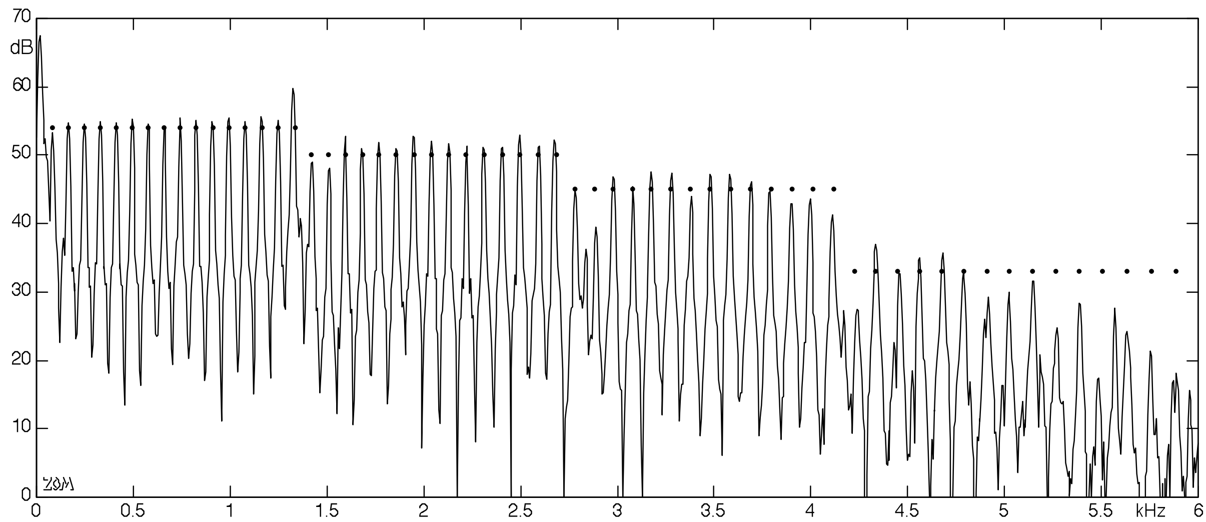

Fig. 1.11.b: Measured spectrum (lines), calculated *spread* partials (dots, b = 1/8500).

The problem mentioned above regarding the selectivity occurs particularly in spectrograms. To generate them, many single spectra are superimposed as color- or grey-scale-coded lines (**Fig. 1.12**). Herein, the level (dB-value) is entered as a function of time (ordinate) and frequency (abscissa). However, a spectrum can never be determined at a *point* in time but only for a time-interval. If we shorten the duration corresponding to this interval in order to obtain a good time–selectivity, the spectral selectivity deteriorates. In Fig. 1.12, the time window has an effective length of 1,9 ms, with the effective bandwidth being 526 Hz. In the low-frequency range, red/yellow bars follow each other with an interval of 12 ms; these are the reflections of the plucking process. The reciprocal of this periodicity corresponds to the fundamental frequency. Towards higher frequencies, the intervals become shorter – corresponding to the spreading of the frequencies of the partials. The quantitative evaluation is not (yet) a good match for Fig. 1.10: as is evident, the inharmonicity occurring towards higher frequencies is much more pronounced on Fig. 1.12.

The reason for these apparent discrepancies is found in the way the analysis is done: a spectrogram shows the envelope shapes corresponding to given frequency ranges, and not the propagation of a certain oscillation phase. For this reason, it is the **group delay** that needs to be considered for the comparison, and not the phase delay. The phase delay is the negative quotient of phase and angular frequency, while the group delay is the negative differential quotient.

$$\tau_p = -\varphi/\omega \qquad \text{Phase delay}$$

$$\tau_g = -d\varphi/d\omega \qquad \text{Group delay}$$

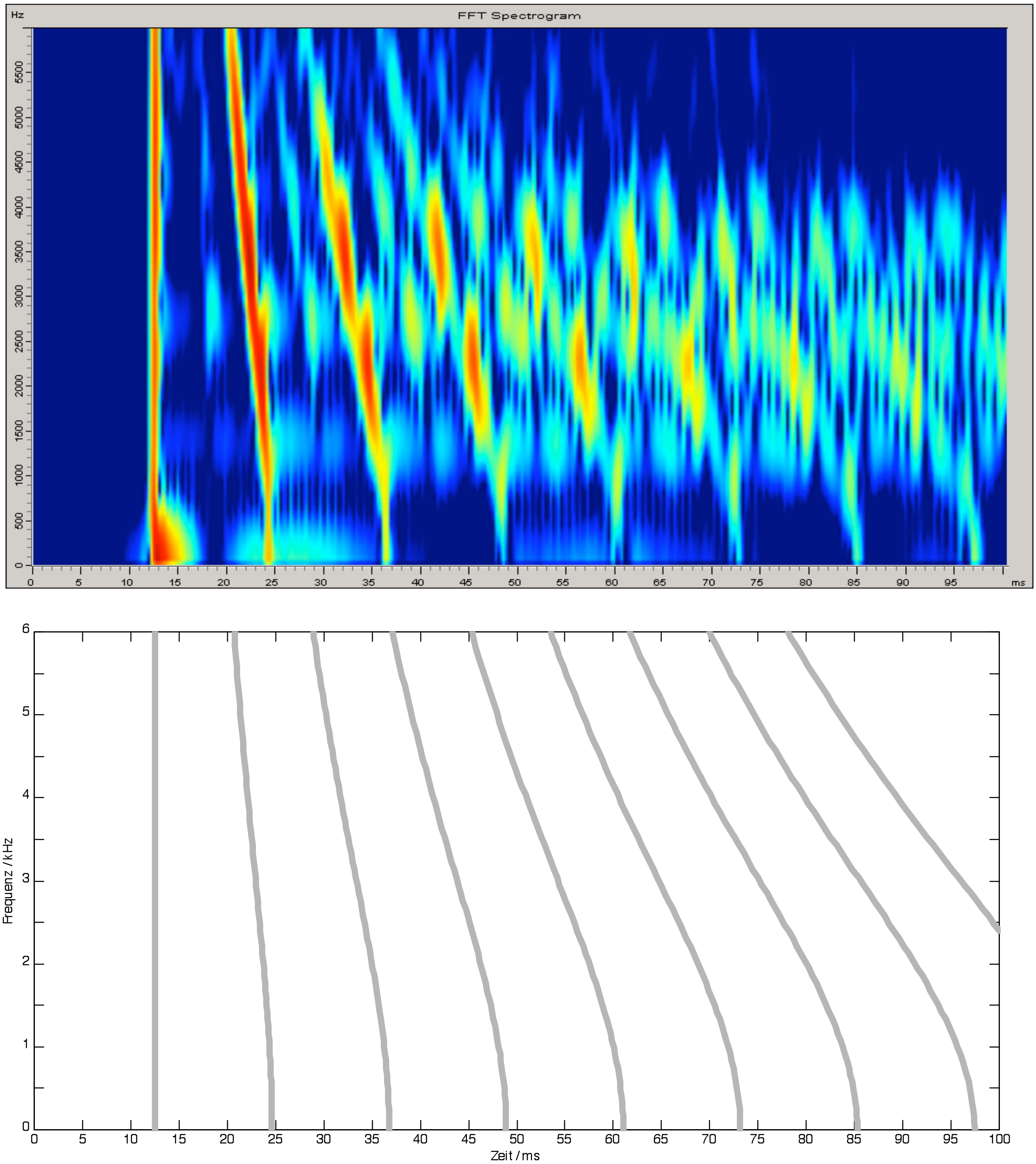

Fig. 1.12: Spectrogram of the plucking process of a low E-string (top); computer simulation (bottom). The resonances occurring at multiples of 1,4 kHz are due to expansion waves (Chapter 1.4). “Frequenz” = frequency.

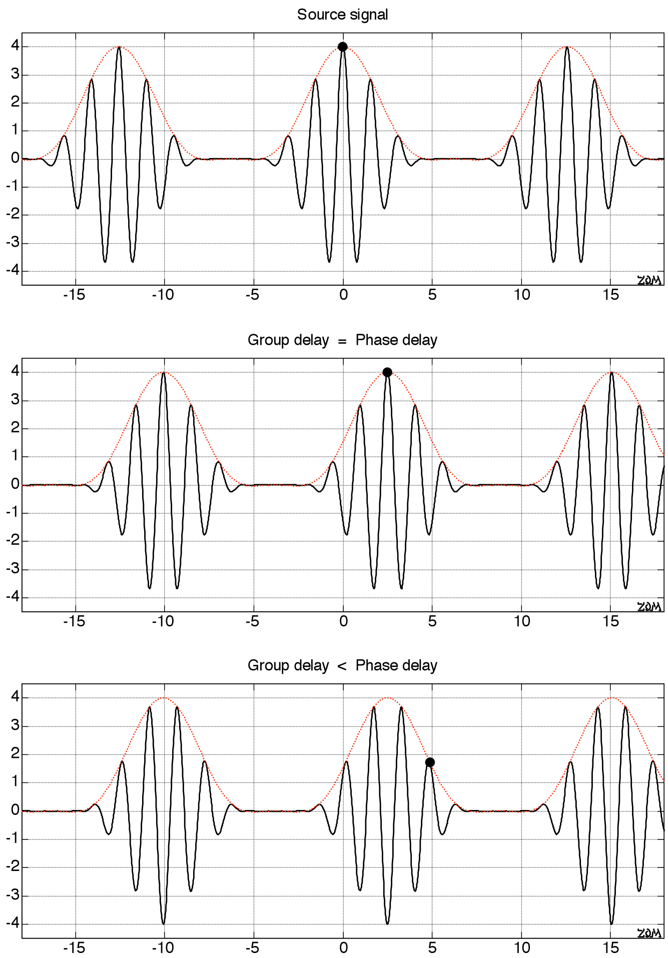

Fig. 1.13 illustrates the differences. The uppermost graph is the time function of a signal resulting from 5 neighboring tones. As this signal runs through a system with frequency-proportional phase, the envelope and the carrier below it are shifted by the same delay (middle graph). Phase delay and group delay are equal in this case.

If there is a linear, but offset relationship, phase- and group-delay differ (lower graph). The envelope is not shifted as much as a certain carrier-phase (marked here with a dot). The time function is not only shifted but has also changed its shape. Due to the frequency-independent group delay, the shape of the envelope has, however, not changed.

Fig. 1.13: Explaining the difference between phase-delay and group-delay.

For a dispersive string, the group delay for a full oscillation period is calculated as:

$$\tau_g = \frac{1}{f_G}\sqrt{\frac{1+\sqrt{1+4b(f_i/f_G)^2}}{2+8b(f_i/f_G)^2}} \qquad \text{for } z = 2L; \qquad \text{Group delay}$$

Inserting into this equation a low value for f_i (e.g. f_G) yields a group delay that is – with good approximation – the reciprocal of the fundamental frequency, i.e. about 12 ms. For higher frequencies this value drops to about 7,8 ms which is a good match to the high-frequency impulse distances observed in Fig. 1.12.

The lower section of **Fig. 1.12**, shows a computer simulation for the spectrogram depicted above it. While the differences are not to be ignored (multiple decay processes of the excited resonances and superimposed expansion waves make for an early unraveling of the original line structure), we can still see already in this simple analysis a good correspondence of the dispersive effects, From the point of view of systems theory, the dispersive propagation may be described as an **all-pass**: a linear, loss-free filter with a frequency dependent delay-time. Compared to an ideal all-pass, the vibration energy of a real string decays – but let's postpone dealing with this effect a bit. Linear filters are described by their complex **transfer function** in the frequency domain, and in the time domain by their impulse response. The **magnitude** of the transfer function of an all-pass is equal to one for all frequencies (loss-free transmission). If the **phase** of the all-pass transfer function were zero, input and output signal would correspond (trivial case). If the phase were proportional to the frequency, all frequency components would be delayed by the same delay time, and the system would not be termed all-pass, but delay line. In a non-trivial all-pass, the phase $\varphi(\omega)$ is not proportional to the frequency. The phase delay thus is frequency-dependent – for a string this occurs in such a way that high frequencies appear at the output of the all-pass after a shorter delay than low frequencies.

Of course, the delay time also depends on the distance traveled. Assuming precise manufacture with place-*in*dependent mass and stiffness along the string, the string represents a **homogenous transmission line**: the propagation speed is frequency-dependent but place-independent. The phase shift thus shows proportionality to the traveled distance – at any frequency (with a frequency-dependent proportionality factor). This assumption corresponds well with the real string; we find somewhat more serious problems with the places of reflection at the nut and bridge … we will have to look into this more specifically later.

It already has been explained with respect to Fig. 1.12 that for the propagation of envelopes it is not the phase delay that is important, but the group delay. In non-dispersive systems, phase delay and group delay are identical, but in the dispersive string the group delay is smaller than the phase delay. As a description of the transfer characteristics of an all-pass, we typically find the **frequency response of the group delay** in the frequency domain, and the **impulse response** in the time domain; both characteristics are equivalent and can be converted one into the other.

The frequency responses of phase delay and group delay are shown in **Fig. 1.14**. The abscissa is the spread-out frequency f_i, rather than the n-fold fundamental frequency.

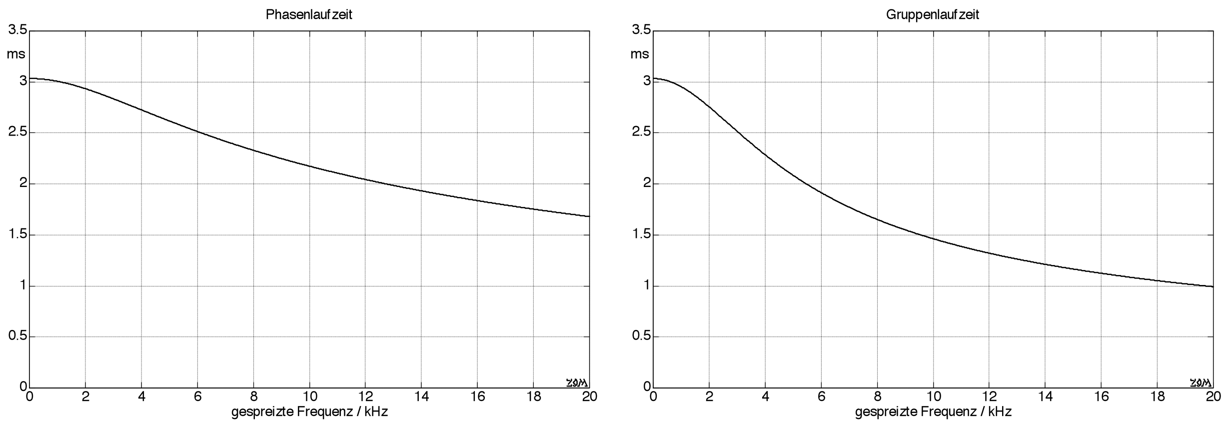

Fig. 1.14: Phase delay and group delay across half the string length (from bridge to mid-string), E_2, b = 1/8000. "Phasenlaufzeit" = phase delay; "Gruppenlaufzeit" = group delay; "gespreizte Frequenz" = spread frequency.

1.3.2 Dispersion in the time domain

Guitar strings are plucked with the finger or a plectrum (pick). A slowly increasing force pulls the string from its rest position, then this force suddenly stops, and the string executes a free damped oscillation. The idealized time function of this excitation is a **force-step**: at the point in time $t = 0$ the force jumps from an initial value to zero. Starting from the plucking point, a step-wave travels in both directions. However, this wave will now change its shape due to the dispersion: the high-frequency components of the step travel faster than the low-frequency ones. The step is being pulled apart in both the frequency- and time-domains. From the viewpoint of systems theory, the dispersive propagation may be modeled by an **all-pass**. The latter is a linear, loss-free filter with frequency-independent transfer coefficient and frequency-dependent delay time (Chapter 1.3.1). Transfer function and **impulse response** represent the transmission-relevant quantities of an all-pass.

The impulse response of a linear system is formed by the inverse Fourier-transform of its transfer function. Convolution of any arbitrary input signal with the impulse response yields the output signal. According to this definition, if the system is stimulated at its input e.g. with a step, the output signal is the result of a convolution of step and impulse response. For this special case, a simplification is possible: the step is the (particular) temporal integral of the impulse. Like differentiation, integration is a linear operation, and therefore the sequence of impulse/integrator/system may be exchanged for impulse/system/integrator (commutative law). The step-response of a linear system therefore corresponds to the integrated impulse response, just like the impulse response corresponds to the derivative of the step response.

The model system used in the following to emulate the plucked string is an all-pass with a step-function being fed to its input.

In **Fig. 1.15.a** we see on the left the measurement result from an E_2-string plucked halfway between nut and bridge ($z = L/2$). On the right, the step-response of an all-pass is shown for comparison. There are clear differences but also some commonalities: the step response permanently switches its polarity after 3 ms; this delay time corresponds to the low-frequency group delay for half the string length. From about 1 ms – corresponding to the shorter high-frequency group delay – we see fast oscillations. In the output signal of the piezo, the high-frequency oscillations have more damping (treble cut). Moreover, there is a dip at 0 – 2 ms caused by the plectrum. After 3 ms, decay processes of the longitudinal resonances appear (Chapter 1.4) – these are not present in the simulation of the all-pass.

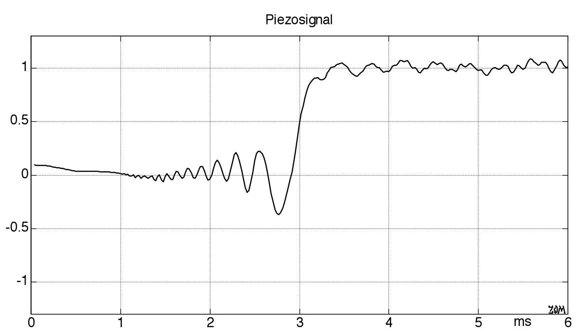

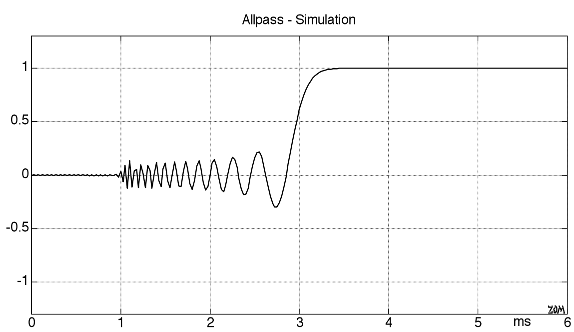

Fig. 1.15.a: Piezo-signal (left) and simple simulation of an all-pass (right); excitation by a step at mid-string and $t = 0$. For the piezo-signal, sign and offset were chosen for best fit.

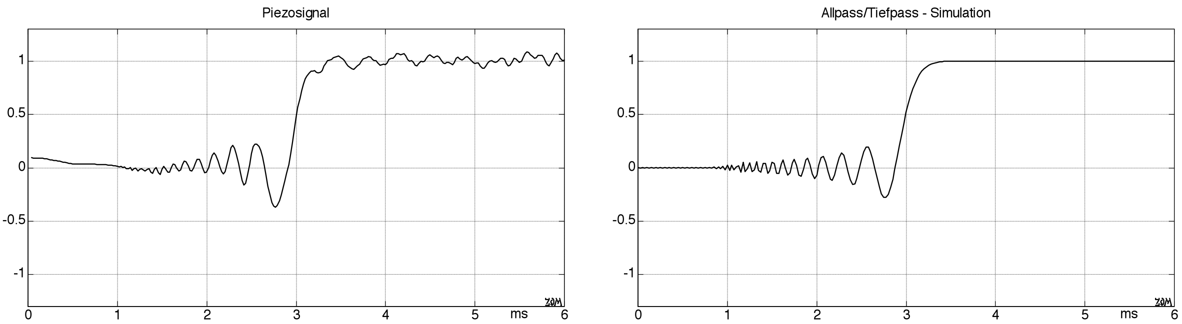

Fig. 1.15b: Piezo signal (left) and all-pass/low-pass simulation; step-excitation at mid-string and $t = 0$. ”Tiefpass” = low-pass.

For **Fig. 1.15.b**, the same all-pass as in Fig. 1.15a was used but supplemented by a simple low-pass in order to model the treble-cut (dissipation). The amplitude of the early oscillations can effectively be damped this way.

Two remarks regarding the **bandwidth**: the piezo-signal was sampled with 48 kHz. It received a band-limitation at 20 kHz by a low-pass filter, just like the all-pass simulation. The lower frequency limit of the measuring amplifier is 2 Hz. DC-coupling is not purposeful and would only crate offset-problems. As a consequence, the zero-point of the ordinate is arbitrary. Moreover, the sign was reversed such that the step happens from zero to positive values as is customary in systems theory.

Fig. 1.16 depicts a longer section taken from the piezo signal. With increasing time, the step is pulled more and more apart, and therefore no “period” is equal to another. Assuming, for one revolution ($z = 2L$), 12 ms at low frequencies and 4 ms for higher frequencies, the step is spread out already across several “periods” after 5 revolutions with 60 ms | 20 ms. A short-term spectrum measured over a short time duration therefore captures signal components that have been reflected differing numbers of times, depending on the frequency range.

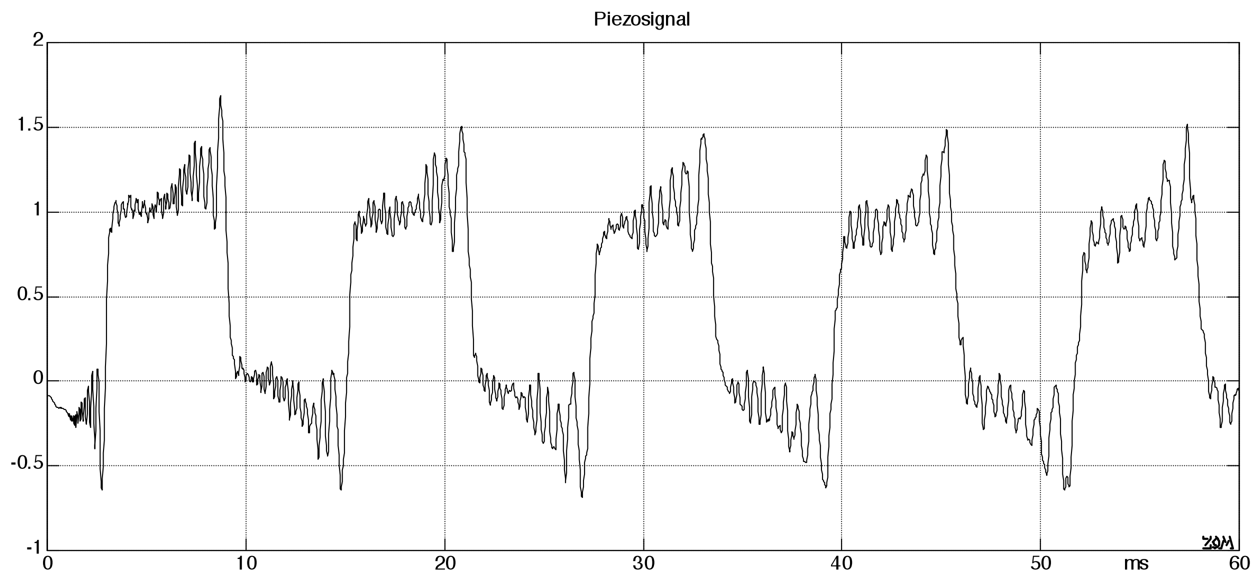

Fig. 1.16: The first 60 ms of the piezo signal; E_2-string, plucked at mid-string with a plectrum.

1.4 Longitudinal waves

For the guitar string, the most important wave type is the flexural wave running along the string with a relatively slow phase speed (Chapter 1.1). However, additional waves may be generated that all have a significantly higher propagation speed but contain – relatively – little energy. Due to the high propagation speed, already their fundamental frequency is relatively high. Still, theses additional waves are worth a look.

In analyses relating to Fig. 1.11, an anomaly at multiples of about 1,4 kHz showed up time and again. At first, this was interpreted as a pickup resonance, until it transpired from supplementary measurements that this irregularity depended on the length of the string. Consequently, not the pickup but the string had to be the source. For bodies with dimensions that are large compared to the structure-borne wave-length, it is known that both transversal and longitudinal waves can appear, and combination-type waves, as well [11]. In long, thin rods we find, on top of the tension-force-dependent flexural waves, mainly **dilatational waves** (extentional waves) manifesting themselves. Their propagation speed is constant and non-dispersive:

$$c_D = \sqrt{\frac{E}{\rho}}$$ Dilatational wave speed

For solid steel strings the math yields $c_D \approx 5100$ m/s; with 64 cm as string length we calculate a (tension-force-dependent) fundamental frequency of about 4 kHz for this dilatational wave.

In **wound strings**, the longitudinal stiffness depends mainly on the diameter D_K of the core, while the mass depends on the outer diameter D_A. Given a length-specific compliance n' and a length-specific mass m', the propagation speed calculates as:

$$c_D = \frac{1}{\sqrt{n' \cdot m'}} = \sqrt{\frac{E \cdot D_K^2 \pi}{\rho \cdot D_A^2 \pi}} = \frac{D_K}{D_A}\sqrt{\frac{E}{\rho}}$$ Dilatational wave speed with winding

Compared to the former formula, the correction factor core-diameter / outer-diameter needs to be considered, as well: for customary strings this ratio is about 0,32 ... 0,42. With the latter number, the fundamental frequency f the dilatational wave decreases to about 1,3 ... 1,6 kHz, – a good fit to the measurements. Even more precise results may be achieved by including both the filling-factor and the stiffness of the winding in the considerations.

The resonances of the dilatational waves can be clearly seen both in Fig. 1.11 (at multiples of 1,4 kHz) and in Fig. 1.15 (after 3 ms). The following model describes the effects on the transmission: when plucking the string, two transversal waves running in opposite directions are generated (Chapter 1.1). The place- and time-dependent field quantities *force* and particle *velocity* are connected via the transmission-line equations (Chapter 2), and the wave impedance of the transversal wave calculates as about 1 Ns/m. The bridge (with its piezo pickup) represents the line termination, it may be seen as a very stiff spring (operation below resonance). The output voltage of the unloaded piezo pickup is proportional to the *displacement* of the bridge. The latter causes a mode coupling, i.e. a small portion of the transversal wave is converted into a dilatational wave. The input impedance of the dilatational-wave line forms a loading of the transversal-wave line and thus influences the transfer coefficient of the piezo pickup.

The termination impedances of the string are seen, as a first-order approximation, as large compared to the wave impedances (for more detailed considerations, neck- and body-resonances would need to be looked into). The input impedance of an open-circuit dilatational-wave line shows a co-tangent-shaped frequency dependency, including maxima at the multiples of the fundamental frequency of the dilatational wave. At these maxima, the possibility of the bridge acting like a spring is impeded, and its displacement (and thus the sensitivity of the piezo pickup) is reduced.

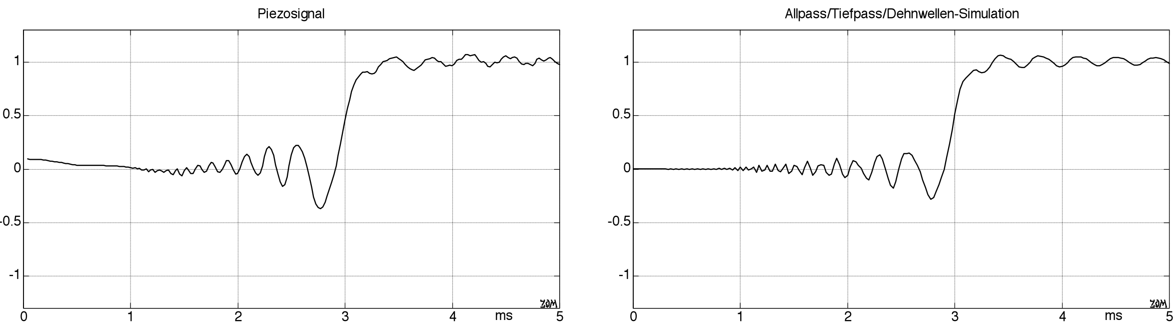

Fig. 1.17: Measurement (left) and dilatational- wave simulation (“Dehnwellensimulation”, right); step-excitation at mid-string at $t = 0$, E_2-Saite. “Tiefpass” = low-pass.

In **Fig. 1.17**, the all-pass simulation was supplemented by a dilatational wave, yielding significant improvement. Any remaining differences are due to the plectrum (low-frequency, left-hand section of the figure) and to reflections at the nut (high-frequency, right-hand section of the figure). Both these effects were not included in the simulation.

The principle effect of the dilatational-wave line on the piezo pickup may be described via discrete elements: at very low frequencies, only the longitudinal stiffness acts, and the model system consists of a spring. To emulate the lowest Eigen-oscillation, the mass is thought to be concentrated in the middle of the string with a spring each left and right of it. Above this resonance, the movement of the mass decreases due to the inertia, and half the spring forms the input impedance. To model the higher Eigen-resonances, the string is subdivided into more and more partial springs with interjacent partial masses. A shortening of the spring corresponds to an increase of the stiffness such that the piezo is loaded by a spring with continuously increasing stiffness as the frequency increases. With this, the piezo-sensitivity decreases towards high frequencies in a staircase-shaped manner, with the steps located at multiples of the dilatational-wave resonances.

In the upper section of **Fig. 1.18**, the spectral analysis of Fig. 1.11 is repeated. The low E-string (E_2) was plucked with a plectrum at a distance of about 5 mm from the bridge. The lower section of the figure shows the result of the simulation calculation, with the dispersion-caused inharmonicity, the dilatational-wave loading, and a simple treble damping (1^{st}-order low-pass) being considered. Both sections of the figure show similar irregularities at integer multiples of 1,4 kHz – these can be explained as **dilatational-wave resonances**. The spectral envelope has a similar shape in both graphs, but differences remain in the details. The most important reason for these differences is in the frequency of the partials, the calculation of which was based on an ideal tensioning of the string in the formulas discussed up to now. The real nut and bridge impedances are, however, not infinite: neck, body, neighboring strings, and many small parts all vibrate as coupled parts of a complicated system. This results in a multitude of structural resonances.

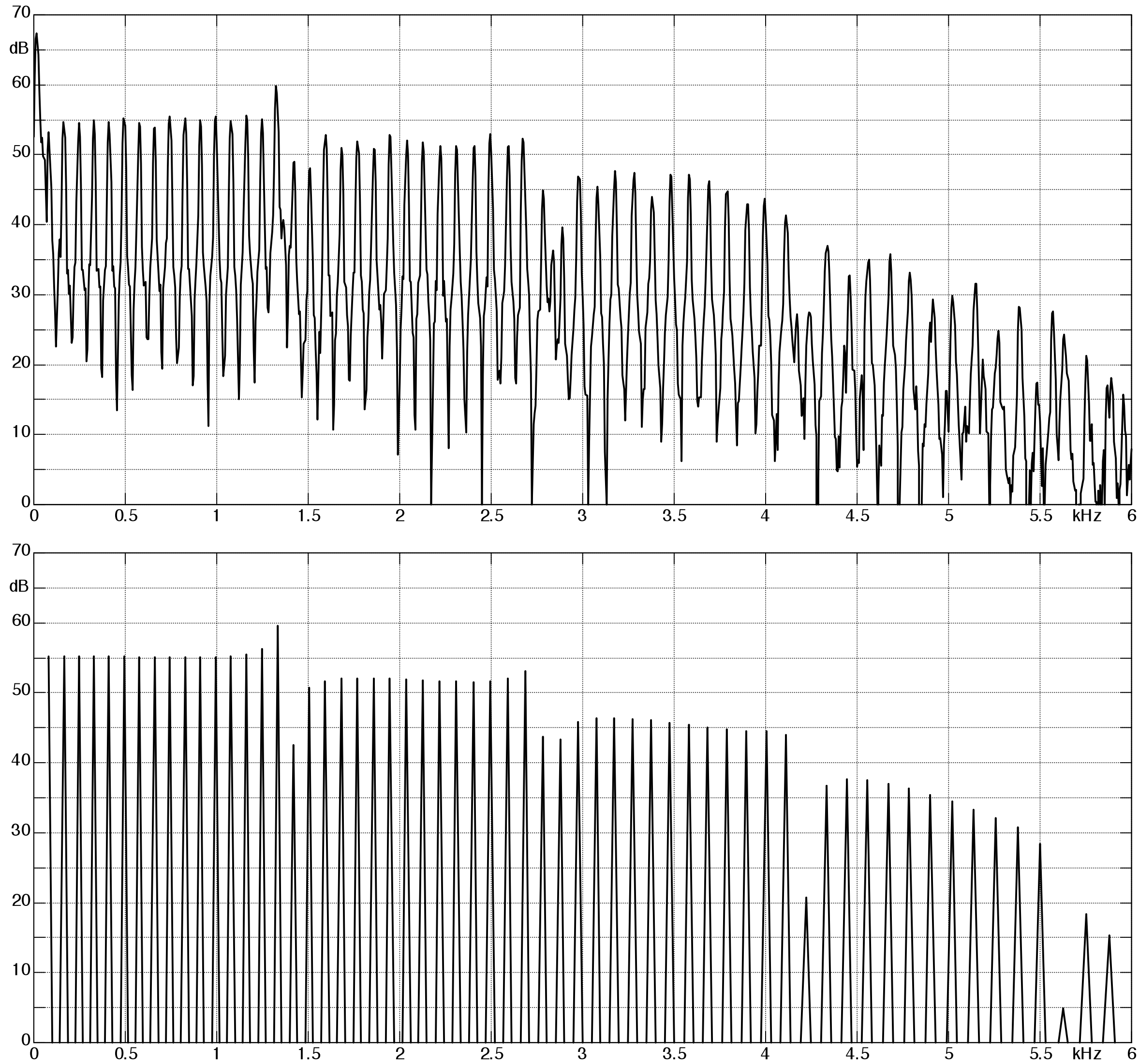

Fig. 1.18: Magnitude spectrum: measurement (top) and model calculation (bottom).

All vibrations may not only appear in one but in three directions – and torsional vibrations are possible, in addition. Not all resonances will substantially influence the bridge impedance but the dilatational waves obviously have a non-negligible effect. In Fig. 1.18, the resonances of the dilatational waves are exclusively considered relative to the frequency response of the piezo (global envelope) – they are not considered regarding their influences on the exact frequencies of the partials (see additional info about this in Chapter 2.5). Because of the high Q-values of the resonances and the connected steep cutoff slopes (dB/Hz), already a resonance-shift of a mere few permille (!) causes a clear change in the levels of the lines. Moreover, additional spectral lines result (clearly visible at 2,8 kHz). The mechanical parameters of a guitar cannot be established with an accuracy of in the permille-range, and thus the limitations of the modeling come into view.

During the investigations, the model based on dilatational waves originated early on as a working hypothesis to explain the step-shaped envelope. Three years later, an experimental setup deploying a laser vibrometer became operational – it delivered further supporting findings:

The laser-based setup consists of stone table weighing in at 250 kg, with a **Polytec laser-head** mounted to it. A steel wire of 0,7 mm diameter is stretched in parallel to the table surface; one end of the wire finds its support in a knife-edge bearing located on a U-brace bolted onto the table surface. The other end of the wire is mounted to an impedance head (Brüel&Kjaer 8001) located on a wall across the hall at a distance of 13,3 m; it measures the longitudinal force. The wire is tensioned such that its fundamental frequency is 5 Hz; given a length of 0,65 m for the string, the equivalent would be a fundamental frequency of 102 Hz. A laser vibrometer sampled the vertical vibration of the wire; the same vibration was also sensed by a pickup mounted under the string on the stone table. This "long string" was excited via a pick made of Pertinax moving downwards in a hammer-like fashion and thus having the effect of a short transversal displacement impulse (**Fig. 1.19**).

With the location of the excitation being close to the bearing of the string, the short section of the string acts like a stiff spring; the long section of the string – with the input impedance being the wave impedance – may be disregarded in comparison. In conjunction with this string stiffness, the mass of the Pertinax pick forms a 2nd-order oscillation system … at least as long as force is being transmitted. Consequently, the string displacement is in the shape of a half-sine in the transversal direction. Fig. 1.19 shows this idealized transversal movement, and also the results of laser-measurements for comparison. Increasing in width due to the dispersion, this half-wave impulse runs along the string as a flexural wave; its group speed (1.3.1) amounts to 133 m/s at low frequencies, and to about three times as much at high frequencies. The first reflection can therefore be expected to be back at the laser vibrometer not earlier than after 66 ms. However, as early as after T = 5,15 ms, the laser beam measures a reflection that is repeated with decreasing amplitude in equidistant intervals. Given an overall running path of 26,6 m, this yields a propagation speed of c_D = 5165 m/s – the typical value for (dispersion free) **dilatational waves** in steel wires.

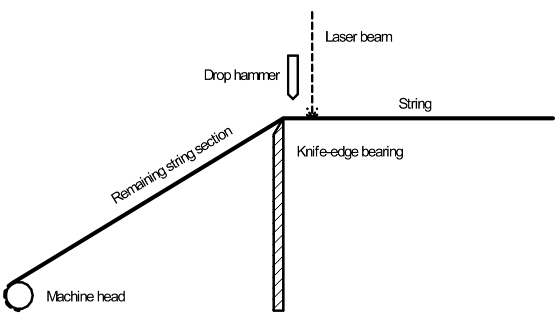

Fig. 1.19: Laser measuring setup (left).
"Wirbel" = machine head; "Saitenreststück" = remaining section of the string; "Fallhammer" = drop hammer; "Schneidenlager" = knife-edge bearing; "Laserstrahl" = laser beam; "Saite" = string;
The graphs shown below depict measuring results of the transversal displacement of the string with different time-axis scaling. Below right: the idealized shape of the curve is indicated as a dashed line and with a horizontal shift. The excitation happens at about 1 mm distance from the knife-edge bearing; the measuring point of the laser is very close to it at 5 mm from the knife-edge bearing. "Auslenkung" = displacement.

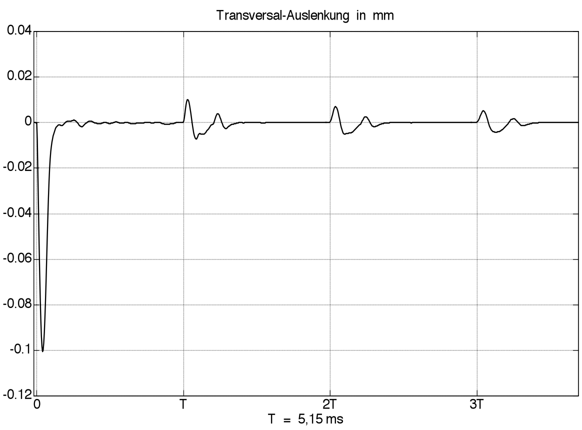

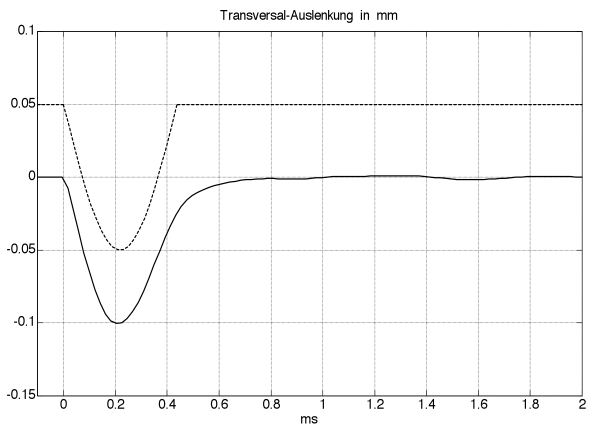

The dilatational wave remains almost invisible to the **laser-vibrometer** because the laser beam can react only to transversal but not to axial movements♣. Periodicities of T = 5,15 ms are nevertheless measured – this is due to a coupling of the two wave types: the string is bent at its bearing, and here the dilatational wave returning after 5,15 ms triggers a secondary flexural wave that is visible to the laser beam.

The measurement results from the laser setup are shown in **Fig. 1.20**, the longitudinal force measured at the end of the string being subject to integration. Without support-bearing, the dilatational wave of the string (having been triggered at the left-hand bearing) reaches the right-hand bearing after 2,6 ms. The excitation impulse is comparable but not identical to the one shown in Fig. 1.19. With the **support-bearing**, the force sensor receives its first excitation after 2,6 ms, as well – there is, however, some attenuation. Without the support-bearing, the second impulse arrives 5,2 ms after the first one, with support-bearing this happens already after 2 ms. The reflection of the longitudinal-force-wave is in phase at both clamps (rigid clamping); at the support-bearing we obtain complex factors for both reflection and transmission. The small ripples visible in the left section of Fig. 1.20 can be traced to unavoidable resonances in the left-hand bearing; they have no special significance.

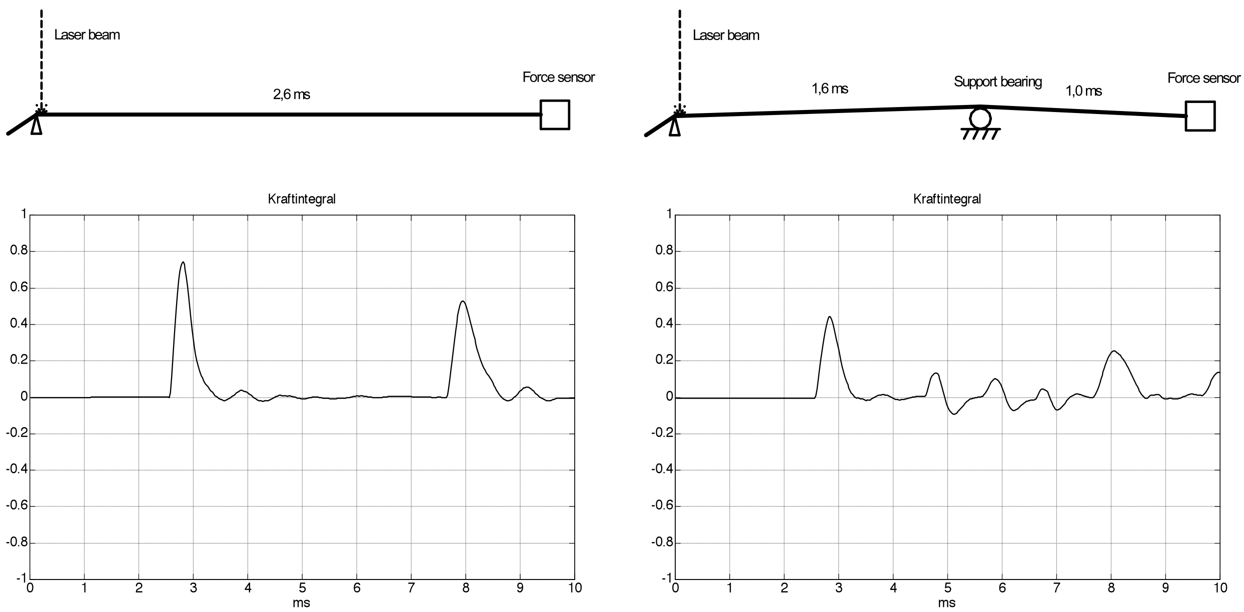

Fig. 1.20: Laser setup with/without support-bearing. The support-bearing separates the string length into two parts 816 cm : 511 cm. The diagrams show the temporal integral of the longitudinal string-force; the unit is Newton · millisecond (Nms). The positive sign indicates that first compression and then strain reach the sensor. "Laserstrahl" = laser beam; "Kraftsensor" = force sensor; "Kraftintegral" = force integral; "Stützlager" = support-bearing.

In the right-hand section of Fig. 1.20, the **reflections** differ (in their shape) from the primary impulse starting at 2,6 ms. Between 4,6 and 7,5 ms, three bipolar impulses can be observed: on its path from the source (at the left-hand bearing) to the force sensor, each of them has traversed the support-bearing once and has additionally received several reflections at the support-bearing. In the case of a uni-polar impulse changing to a bi-polar one, we can assume high-pass filtering. The change of shape of the impulse allowed only for the conclusion that the reflection acts as a **high-pass**, and the transmission as a **low-pass**.

♣ Effects of lateral contraction are too weak.

Fig. 1.21 shows results of calculations using a **dilatation-wave model**. A 1st-order low-pass (cutoff frequency at 1,5 kHz) emulates the transmission across the support bearing, while a 1st-order high-pass (cutoff frequency at 1,5 kHz) models the reflection. The cutoff frequency was determined via "curve-fitting" (vulgo: we tried until we got a match). The agreement is remarkable.

This figure is reserved for the print version of this book

This figure is reserved for the print version of this book

Fig. 1.21: Measurement (left) and model calculation (right); string <u>with</u> support-bearing, as in Fig. 1.20. The time "zero" is shifted by 2,6 ms to the start of the first impulse. The lateral string displacement determined via the laser (close to the left-hand bearing) was used as the input signal for the model calculation.
"Kraftintegral" = force integral.

A movable brass-cylinder (∅ 4 mm) served as **support-bearing** (Fig. 1.20), with the string forming a bend angle of 5° around it. Using the parallel-axes theorem, the axial moment of inertia of a cylinder ($mD^2/8$) can be recalculated into the generatrix moment of inertia ($3mD^2/8$), with m = mass and D = diameter. Longitudinal movements of the string roll the cylinder back and forth on its base; propelling force is the torque $F \cdot D$, with F = longitudinal force in the string. With respect to the longitudinal movement of the string, the inertia of the rolling movement of the support-bearing can be recalculated into an equivalent translation using the equivalent mass $m_ä = 3m/8$. Here, m is the actual mass of the cylinder (volume x density), and $m_ä$ is the equivalent mass to be shifted from the point of view of the string. The source impedance of the dilatational wave arriving at the support bearing is the impedance of the dilatational wave. Given a steel wire of a diameter of 0,7 mm, Z_W is about 15,8 Ns/m (see appendix). The wave transmitted across the support bearing also forms a loading of the latter with Z_W. The support-bearing itself is described via the equivalent mass (**Fig. 1.22**). Using this, the cutoff frequency of the low-pass results as: $f_x = 1/(\pi C R_W) = Z_W/(\pi m_ä)$, and the equivalent mass may be calculated as 3,4 g. From the latter, the **mass of the cylinder** follows: m = 8,9 g. The cylinder used in the experimental setup indeed had a mass of 8,5 g – the results of the model are nicely confirmed. Whether the cutoff frequency is set to 1500 Hz or 1578 Hz will change the curves in Fig. 1.21 by merely by the width of a stroke.

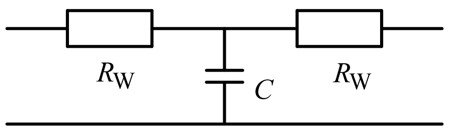

Fig. 1.22: Electrical analogous circuit [3] of the support-bearing. The mechanical wave impedance is transformed into an electrical conductance; the equivalent mass is transformed into a capacitance (FI-analogy).

The reflection- and transmission-processes may also be calculated using the equations for the transversal wave given in Chapter 2.5; in this case the parallel connection of R_W and C needs to be taken for the bearing impedance: $r_F = R_W \cdot pC/(2 + R_W \cdot pC)$. This corresponds to a high-pass HP1.

In order to localize the **origin** of the dilatational wave, the string was plucked at a distance of 51 cm from the left-hand string bearing (**Fig. 1.23**). If already the impact of the drop hammer onto the string would trigger a dilatational wave, then the measured force integral would have to be a dispersion-free image of the string displacement at the location of the origin. However, the result is in fact a better match to the displacement measured closely to the bearing – the only conclusion being that the main portion of the dilatational wave is generated only at the time when the (dispersively broadened) flexural wave has reached the left-hand bearing. This hypothesis is supported by the delay times depicted ion Fig. 1.23, as well.

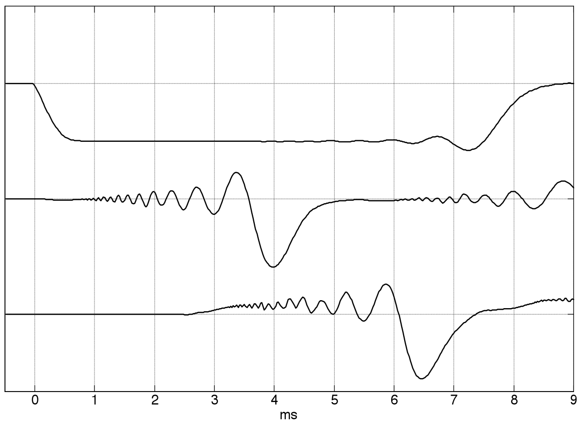

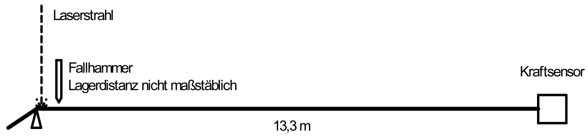

Fig. 1.23: (top to bottom)
- Transversal displacement at the left-hand plucking point,
- Transversal displacement at the left-hand string bearing,
- Integral of the longitudinal force at the right-hand string bearing

Conclusion: dilatational waves merely make for 2nd-order effects on a guitar, but their influence may not be entirely neglected, either. The plucking action mainly generates a flexural wave – but as soon as this hits a bearing (nut, bridge, fret), part of the flexural wave-energy will be transformed into a dilatational wave. Dilatational waves propagate without dispersion and create resonances in the frequency range above 1 kHz. A bearing with a small surface towards the string will only partially reflect a dilatational wave; part of the dilatational wave-energy will be transmitted across the bearing into the other part of the string. The reflected portion manifests itself partially as a dilatational wave and partially as flexural wave.

Fig. 1.24 shows the significance of this **mode-coupling**: a string of 13,3 m length was plucked close to its left-hand bearing, with the laser measuring-point right next to it. At 20 cm from the plucking position, a Telecaster pickup (electrically loaded with 110 kΩ // 330 pF) was mounted below the string. The integral of the pickup voltage is shown in Fig. 1.24 in normalized fashion. The flexural wave passes the pickup 1 ms after its generation and induces a voltage there. The dilatational wave that is also generated runs along the string, is reflected, and arrives back at the bearing after 5,2 ms. Here, a secondary flexural wave is generated (among other waves) that passes the pickup after another millisecond. In Fig. 1.24, the maximum of this secondary impulse reaches almost 40% of the magnitude of the primary impulse. At least for this experimental setup, this is an impressive testimony for the significance of the dilatational wave.

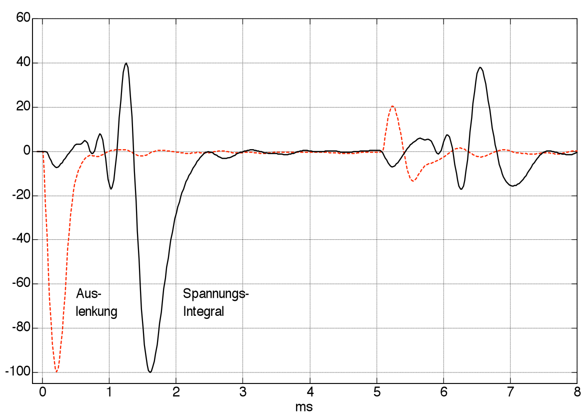

Fig. 1.24: Measurments with a magnetic pickup. “Auslenkung” = displacement; “Spannungsintegral” = voltage integral

1.5 The plucking (or picking) process

The guitar string is plucked (or picked) with the finger (-nail) or a plectrum (pick, fingerpick). The following calculations and measurements describe the excitation with a pick because this represents the dominating approach for electric guitars.

1.5.1 Dispersion-deconvolution

Compared to the (particle) velocity of the string, the speed of the pick is relatively slow; in fact, the displacing of the string can be regarded as quasi-stationary. For low-frequency movements, the string acts as a spring with a lateral stiffness s_Q (depending on the scale *M*), the tension force Ψ, and the distance x between location of picking and bridge:

$$s_Q = \frac{\Psi}{M} \cdot \frac{M/x}{1 - x/M}$$ Lateral stiffness

Usually, the location of picking is about 6 – 10 cm from the bridge, with a lateral stiffness of about 1000 – 2000 N/m resulting. Given a typical displacement of 2 mm, the potential **excitation energy** will be around 2 – 4 mWs. No significantly higher energy levels will be obtainable due to the distance of string to fretboard, but lower energy levels may certainly occur with light plucking. Because the lateral stiffness is similar for all 6 strings, the excitation energy of all strings is comparable, as well.

First, the string converts the excitation energy into vibration energy that is on the one hand radiated as airborne sound, and that on the other hand will directly be converted into heat energy. If all of the vibration energy would remain within the string, the latter would heat up by about 1/1000th of a degree – no really much at all. A well-built acoustic guitar will convert a considerable portion of the vibration energy into airborne sound: in an anechoic chamber, peak sound pressure levels of just shy of 90 dB may be reached at 1 m distance. Measurements with a Martin D45V yielded an **airborne sound energy** of about 1 mWs. This, however, represents merely an orientation because beaming and plucking strength were not determined precisely – indeed the investigation of acoustic guitars is not the actual aim here.

When analyzing the string oscillation from an instrumentation-point-of-view, several systems need to be distinguished: generator, string, and pickup. The **generator** describes the string excitation. Idealized, the plucking delivers a force-step, but in reality differences to the ideal step are found depending on the movement of the pick. For the first few milliseconds, the **string** may be described quite well as a loss-free, dispersive, homogeneous transmission line; for more extended observations, damping increasing towards high frequencies needs to be considered. The **pickup** converts mechanical vibrations into electrical signals. Its sensitivity depends on the oscillation plane of the waves, and moreover we encounter strong frequency dependence. The term “pickup” shall here be used rather broadly at first; it includes all frequency dependencies that are not directly due to the plucking process or to the flexural wave. A distinction into further subsystems may be necessary – depending on the circumstances.

The objective of the present investigations was to describe the transmission behavior of the above systems. Since all three subsystems interact (the plucking process cannot be analyzed without the string, the pickup will re-act towards the string), an isolated system analysis was not possible. In some respects, the vibration instrumentation also provided limitations, in particular if measurements up to 10 kHz or even 20 kHz are targeted.

The below measurements were taken with the Ovation Viper already mentioned. The string was plucked with a **plastic plectrum** given realistic conditions (in situ). This provided, as a first approximation, a step-shaped imprinted force; however, more precise investigations show significant deviations from this. The problem is not so much the actual **step** itself (which of course may not be of infinitely fast speed: natura non facit saltus), but much more the way the force develops ahead of the actual step. First, the plectrum relatively slowly presses the string to the side. Just before the step, a relative movement between string and plectrum commences which may in turn include both sliding friction and static friction (slip-stick). In this, the force fluctuates quickly. After the plectrum separates from the string, it moves according to a damped Eigen-oscillation (natural vibration) that may include another short contact to the string. It is almost impossible to directly measure the forces occurring at the tip of the plectrum – especially not up to 20 kHz. However, the piezo-signal allows for conclusions regarding the excitation signal.

To describe it, the overall transmission line is divided into three subsystems: the **plectrum-filter** that forms the real force transmission from the ideal step, the **string-filter** modeling the dispersive flexural-wave propagation, and the **piezo-filter** emulating the transfer characteristic of the pickup (incl. connected resonators). If on top of the step-transmission, the reflections are of interest too, a recursive structure is required (Chapter 2.8).

The individual filters are taken to be linear – this should be a correct assumption at least for light plucking of the string. Moreover, the piezo-filter is of time-invariant character. The string definitely does not have that quality: an old string features a much stronger treble-damping than a new one. Within a single series of experiments, however, the string may be seen as time-invariant as long as no detuning occurs. The plucking process is difficult to repeat the exact same way; it is time-variant, as well. Using suitable mechanical contraptions, an acceptable (albeit not ideal) reproducibility is possible.

The overall system between step-excitation and piezo-signal is described via an overall transfer function and a step response (or impulse response). Without supplementary knowledge, a division into the individual subsystems is not possible. Assuming restricted conditions, it is, however, possible to determine approximated transfer characteristics.

First considerations are directed towards the wave propagation. The frequency dependence of the group delay could already be shown using short-term spectroscopy, with good agreement between physical explanation (cantilever) and measurement. The measurements of the evolution of the levels of the partials during the first milliseconds indicates only very little damping; therefore assuming a loss-free all-pass is justified.

The following considerations relate to the low E-string plucked in its middle with a plectrum. While the step runs from the middle of the string, the levels of the partials do not change, but the phases are shifted such that the step is spread out (Fig. 1.16). If we shift the phases back using an inverse filter, the step reappears. It is changed by the piezo-filter, though, and after a short time, the saddle reflections superimpose themselves (**Fig. 1.25**).

Shifting back the phases corresponds to a de-convolution using the impulse response of the all-pass, or a multiplication with the inverse transfer function of the all-pass. We need to consider here that a de-convolution is only possible for one single line-length (e.g. $L/2$), and for this reason the steps following later on the time-axis in Fig. 1.25 still show all-pass distortion. Due to the de-convolution, the step spread out across the time range from 1 – 3 ms is concentrated to the zero point on the time axis. The signal occurring ahead of that is the excitation by the plectrum, convolved with the impulse response of the piezo-filter. Now, this is where things get complicated: the plectrum-filter and the piezo-filter cannot be separated without any further assumptions. There are an infinite number of possibilities to separate a product into two factors.

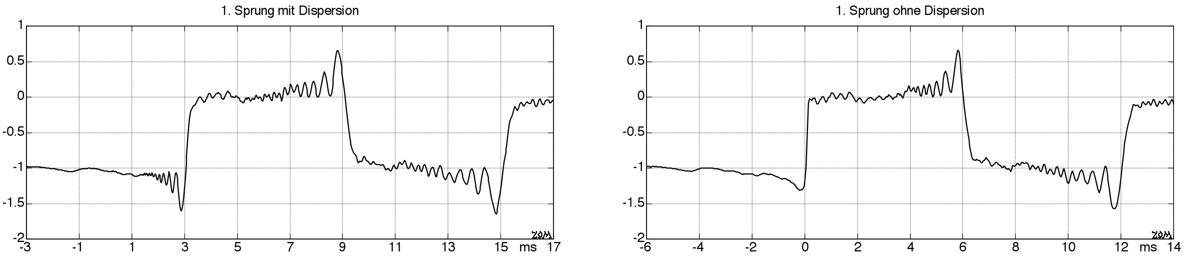

Fig. 1.25: Original piezo-signal (left), de-convolved piezo-signal (right); low E-string plucked in the middle. “1. Sprung mit/ohne Disperion” = 1st step with/without dispersion.

However, in order to fundamentally understand the plucking process, an exact system-separation is not necessary in the first place. We already obtain a good approximation from defining the signal shape ahead of the first step as the plectrum-excitation. For a more exact analysis, measurements with the laser vibrometer are being prepared.

Already a simple evaluation of many plucking processes reveals various mechanisms influencing the vibration:

The distance between plucking location and bridge is responsible for characteristic comb-filters; this will be discussed in-depth later.
Shape and hardness of the plectrum influence the treble response.
The attack angle of the plectrum influences the bass response.
Bouncing and “slip-stick” processes lead to comb-filtering.

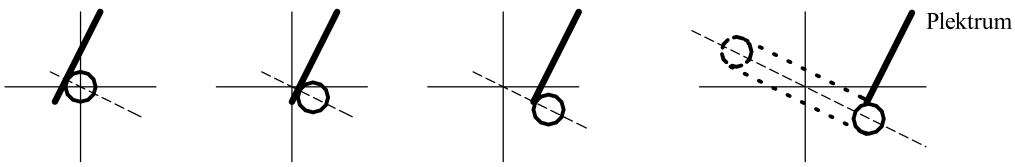

Fig. 1.26: String movement fro friction-free plectrum excitation; guitar top horizontal (sectional image). “Plektrum” = plectrum.

In **Fig. 1.26** we see (from left to right) four consecutive points in time of an excitation process. The guitar top is horizontal and the plectrum is steered in parallel to it. On the left, the plectrum touches the string without transmission of any force. In the second figure, the string is displaced along a line perpendicular to the plectrum and running through the zero position of the string. In the third figure, the displacement progresses, and in the fourth figure the string just starts to leave the plectrum and vibrate along the dashed path. The whole process is taken to be free of friction.

Given constant horizontal plectrum-speed a sawtooth-shaped string displacement results. A piezo-pickup built into the bridge will react mainly to movements normal to the guitar top (as will your usual magnetic pickup with coils), and therefore only the vertical vibration is of any significance. With slow plectrum movement, the string acts as a spring. The vertical force is proportional to the vertical displacement, and both increase time-proportionally up to a maximum value. The excitation force then instantly breaks down to zero.

In reality, the plectrum will not move precisely in horizontal fashion. Rather, contact forces will deflect it upwards. Moreover, its angle of attack will change, and for thin plectra bending will occur in addition. The sliding friction between string and plectrum also allows for small deviations from the dashed line, and there might be stochastic **slip-stick** movements. The latter stem from the difference between sliding friction and static friction: if the plectrum-parallel string force becomes greater than the static friction force, a relative movement between string and plectrum sets in along the plectrum. Since the smaller retention force is now substantially surpassed, the string can slip over a small distance – until it is stopped again via the (higher) static friction force.

For Fig. 1.26, the plectrum is angled at 63° relative to the guitar top, but remains parallel to the longitudinal axis of the string. The smaller this angle of attack becomes, the easier it is for the string to continuously slip towards the bottom. Increasing this angle to 90° (i.e. the plectrum is perpendicular to the guitar top), the string is displaced only horizontally at first – there is no vertical movement. It some point the plectrum has to yield, though – either it boggles towards the top, or it bends or changes its angle such that the string can move downwards. The associated excitation impulse has a shorter duration compared to the angled plectrum: the "boggling" can happen only during the very last millisecond, so to say.

If the plectrum is not held exactly in parallel to the longitudinal axis of the string but at a slight angle, the friction changes. This is because the string does not slide along the surface of the plectrum anymore but skips along the edge of the plectrum. In most cases, the edge is rough – which increases the stochastic component in the excitation. The latter effect is further increased for wound strings.

Therefore, the guitar player has many possibilities to influence the excitation impulse – and thus the sound of the guitar. This begins with the choice of the pick, its free length, and its angle relative to the guitar top and relative to the longitudinal axis of the string. In addition to the plectrum, the fingertip may contact the string during the plucking process (teeth have also been know to get used here …), and on top of it all the location of the plucking may be varied, and the strength of the plucking, of course.

A simple, step-shaped excitation is conducive to the system-theoretical description of the string. Since moreover the evaluation of its reproducibility is done with relative ease, this excitation was the basis for many measurements. However, that does not mean that the ideal step-excitation represents the desirable objective for the guitarist.

1.5.2 Influence of the plectrum

It is most purposeful to discuss the effects of the plucking process on the sound in the frequency domain (**Fig. 1.27**). The force impulse shown in the figure has an arbitrary duration of T = 80 ms; $\hat{F}$ is the maximum value (negative in the present case). F_S describes the spectrum corresponding to this sawtooth impulse, and F_δ pertains to the time-derivative of the sawtooth impulse. Within the frequency range pertinent to the guitar it makes no big difference whether the impulse starts at –80 ms (as it does in the figure) or much earlier … it is only important that the actual step occurs at t = 0. For this reason, we use the term **step excitation** despite the fact that strictly speaking we have an impulse. We obtain the mathematically correct limiting case as T moves towards ∞; the first fraction in the spectral function vanishes in this case and – with $1/j\omega$ – a pure (rectangular) step-function remains. The time-derivative of this ideal step is the **Dirac impulse** that corresponds to a constant (white) spectrum F_δ. In systems theory, (Dirac-) impulse excitation and impulse response are most commonly used; step excitation and step response are somewhat closer to the practical application. Disregarding the frequency f = 0 that does not actually exist, both descriptions are equivalent and may be converted from one to the other.

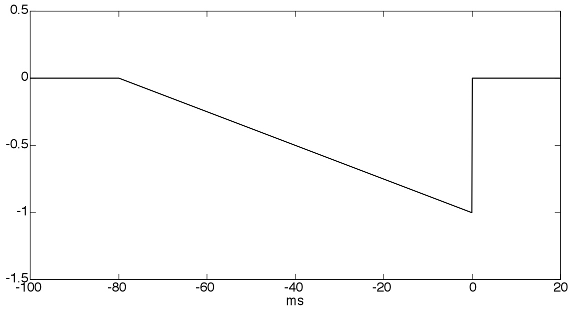

$$F_S(j\omega) = \hat{F}\left(\frac{1-\exp(j\omega T)}{\omega^2 T} - \frac{1}{j\omega}\right)$$

$$F_\delta(j\omega) = \hat{F}\left(j\frac{1-\exp(j\omega T)}{\omega T} - 1\right)$$

Fig. 1.27: Sawtooth impulse: time- and spectral-function

Because in reality the force process occurring upon plucking does not correspond to the depiction in Fig. 1.27, we define a **plectrum-filter** that shapes the actual force process from the theoretical rectangular step. The magnitude of the frequency response this plectrum-filter has describes the impact of the plucking process onto the sound.

The following figures show the analyses for the already mentioned Ovation guitar. The low E-string was plucked with a thin nylon-pick (Meazzi 19), while the piezo-signal was fed directly into a high-impedance measuring amplifier – and cleared of the dispersion via de-convolution with an inverse all-pass (Chapter 1.3.2) **Fig. 1.28** shows two time functions obtained that way. Compared to Fig. 1.27, there are several striking differences: the force increase (in terms of its amount) is not linear but progressive; during the last few milliseconds several peaks appear (slip-stick); after the step, reflections are visible that presumably are caused by longitudinal resonances.

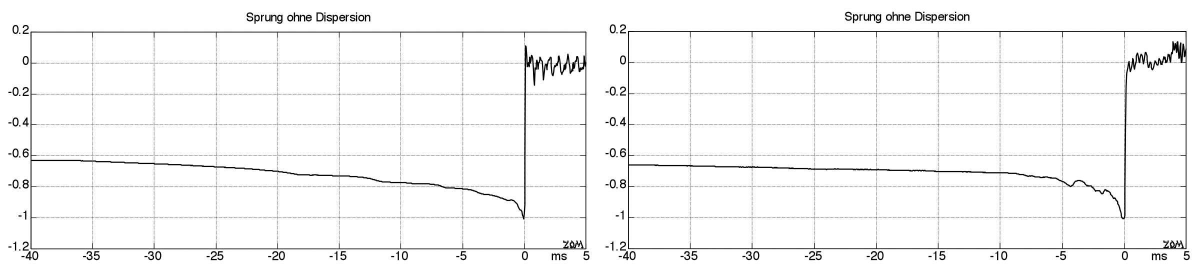

Fig. 1.28: De-convolved piezo-signal; two different plucking processes.
"Sprung ohne Dispersion" = step without dispersion.

In **Fig. 1.29** we see different plucking processes in comparison. The left-hand column shows the dispersion-free, de-convolved piezo-signal while the right-hand column shows the magnitude spectrum belonging to the differentiated piezo-signal. The derivative makes for an easier evaluation: the ideal rectangular step is linked to a constant (white) spectral function.

The first line a) depicts an almost perfect step. Only from about 3 kHz, a treble loss occurs; it is connected to the rounding off of the step. There may be several reasons for this: the tip of the plectrum is rounded off, and therefore the string is not displaced in an exactly triangular manner. This effect is probably further increased by the bending stiffness of the string. The high frequencies are consequently attenuated already in the excitation signal. In addition, dispersion effects in the string need to be considered that also manifest themselves in the high frequency range.

In the case of b), the force rises to its magnitude maximum only during the very last milliseconds. This will occur if the plectrum has a high angle of attack and moves in parallel to the guitar top. The shape is more impulse-like, and in the spectrum the bass is attenuated.

The analyses c) to e) indicate a progressive treble damping as it is typical for a round, hard plectrum.

For the remaining analyses, the force increases first (in its magnitude) and then moves through a magnitude minimum (the force acts in the negative direction). Presumably, this includes a sliding along the string of the plectrum, the latter getting stuck on the string for a short time and then finally separating from the string.

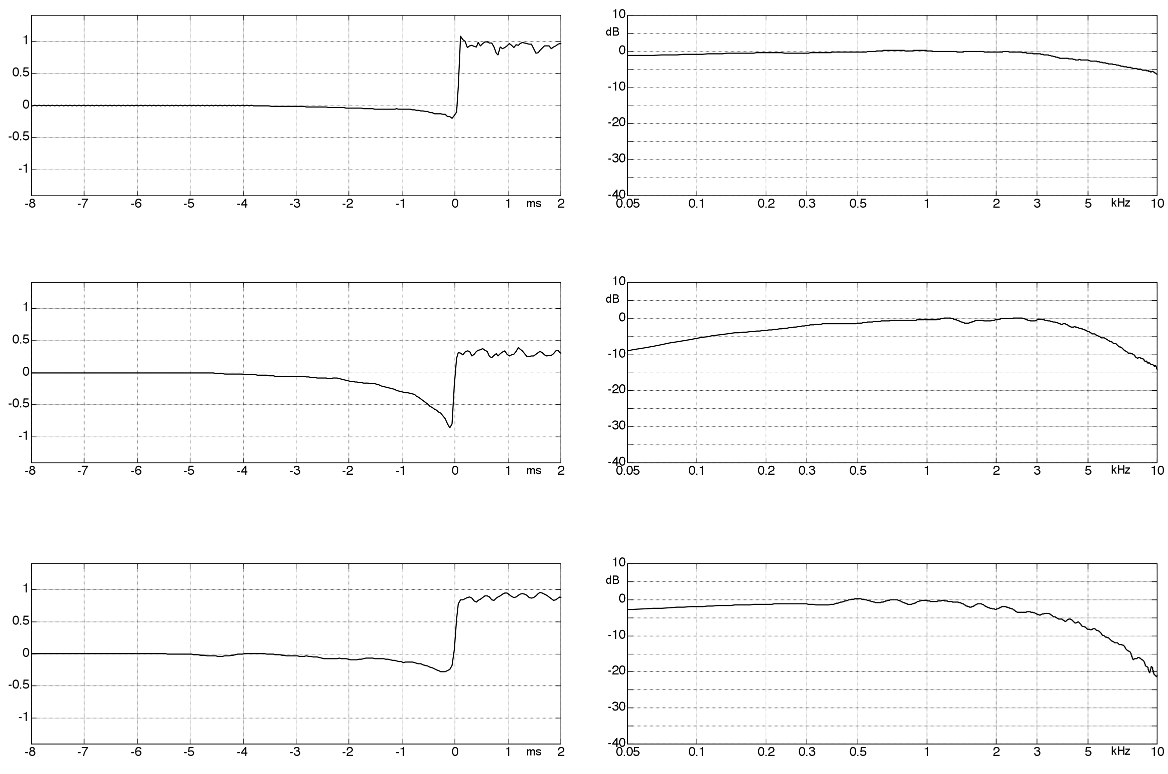

a)

b)

c)

Fig. 1.29: Excitation step, and spectrum of the differentiated step for various plectrum movements.

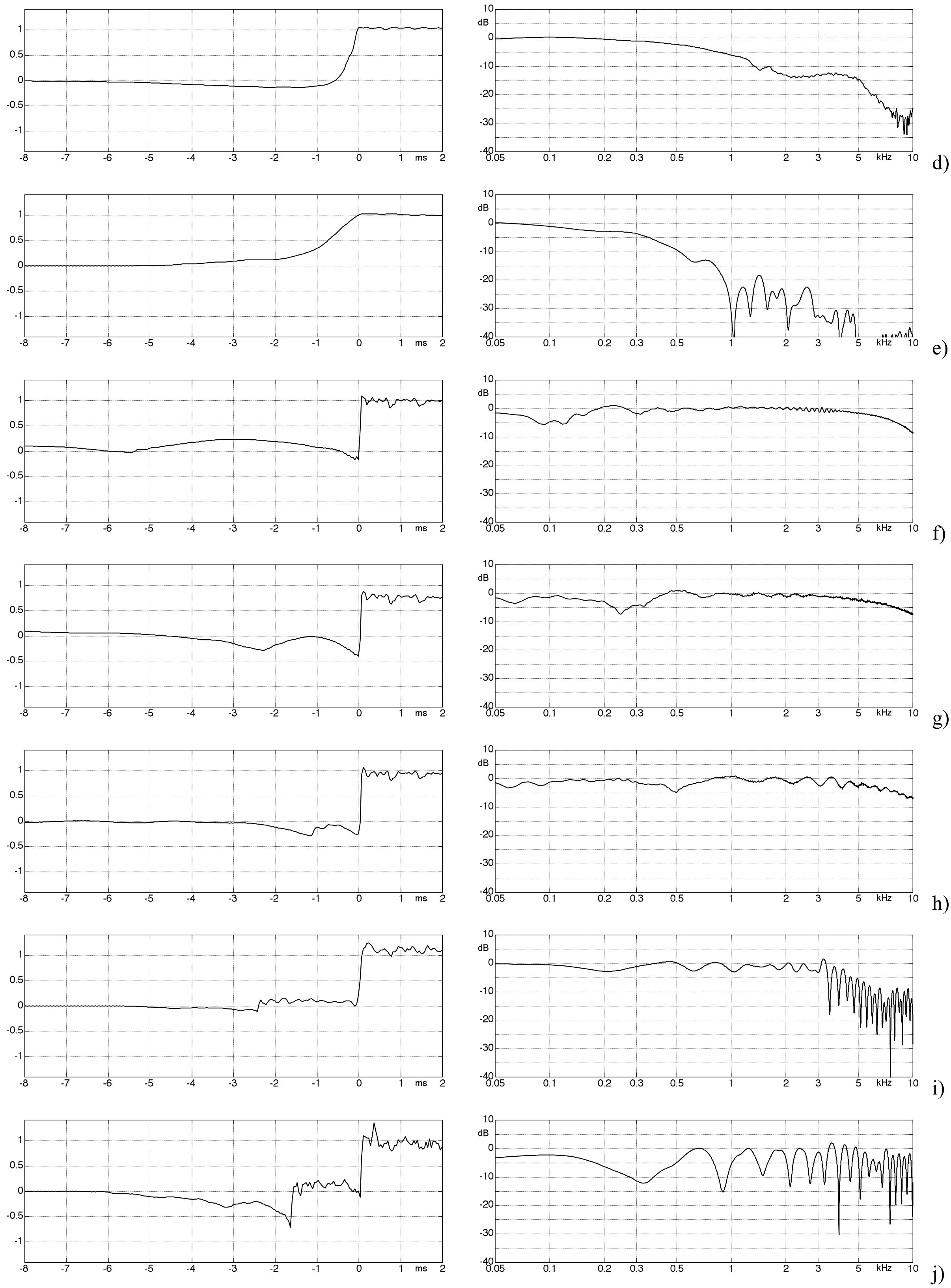

Fig. 1.29: Continuation from the previous page.

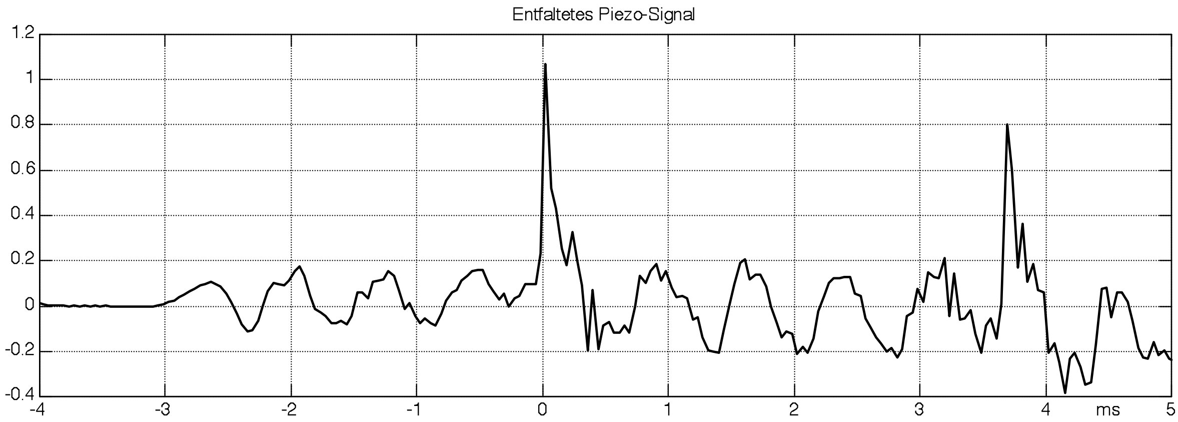

Fig. 1.30: De-convolved piezo-signal for the string excited in its longitudinal direction (scratched string). "Entfaltet" = de-convolved.

Fig. 1.30 documents an interesting detail: here, the low E-string was excited using a sharp-edged metal plectrum at mid-string in the **longitudinal direction**, i.e. the plectrum scratches along the string, jumping from one winding to the next. The signal transmitted by the piezo was again de-convolved i.e. cleared of the dispersion. As the plectrum jumps across the winding, a flexural wave is generated. The first (de-convolved) impulse of this wave is shown at 0 ms (the second impulse appears at 3,7 ms). However, in addition a **dilatational wave** of about 1,4 kHz occurs (Chapter 1.4). This (non-dispersive) dilatational wave propagates with a considerably higher speed than the transversal wave; its start is shifted by 3 ms towards the past due to the de-convolution. In fact, the de-convolution algorithm does separate according to wave-type but it corrects the phase delay of any 1,4-kHz-signal by -3 ms. Further details of the dilatational wave (in particular regarding its coupling to the transversal wave) have already been described in Chapter 1.4.

The plucking processes shown in Figs. 1.29 and 1.30 are typical for guitars but represent merely a relatively arbitrary selection. There is also a multitude of other possibilities to excite the string – and we need to particularly consider that the tip of the thumb or the first finger may also come into contact with the string. It is therefore not necessarily an indication of excessive vanity if the well-known professional guitarist, after an extensive narrative highlighting his wonderful custom-built paraphernalia, concludes the interview about his equipment with a confident: "90% of the sound is in the fingers, though".

1.5.3 String-bouncing

If a string is plucked with little force, it will approximately react as a linear system. This means that doubling the initial displacement will also double the displacement at any instant of the subsequent vibration process. Of course, any displacement is limited – at some point the string will hit the frets on the fretboard. In doing so, it generates a somewhat rattling, buzzing sound. To some degree, this is in fact a means of musical expression and thus not something generally undesired.

In the book "E-Gitarren" by Day/Waldenmaier we find the recommendation: "A slight tilt of the bridge makes it possible to adjust the action of the high E-string a little lower than that of the low E-string. The latter has a more pronounced vibration amplitude and requires more space that the high strings ". However, the transverse stiffness for all customary string sets is higher for the low E-string (E_2) than it is for the high E-string (E_4) – why then would the stiffer string require more space for its vibration? It is o.k. to concede this space to it; that decision is, however, just as individual as the choice of the string diameter and cannot be justified with a generally larger amplitude.

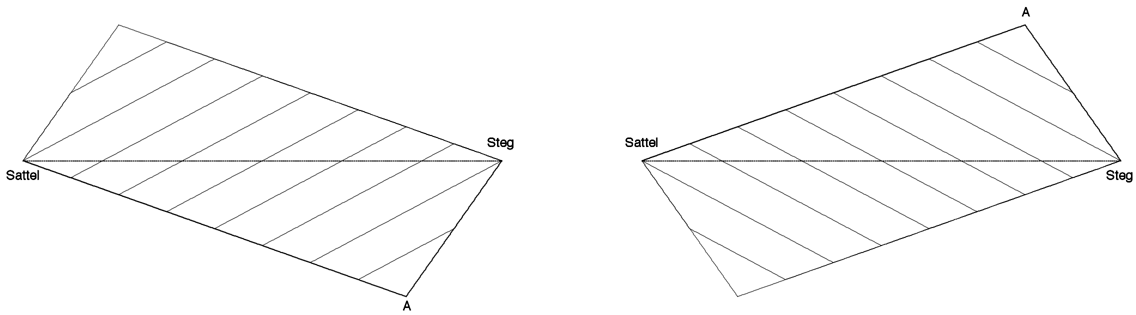

Fig. 1.31: String displaced at A (bold line), intermediate positions of the vibration (thin lines). In the left-hand figure, the string was pressed to the guitar body and then released, on the right it was pulled up and released. "Sattel" = nut; "Steg" = bridge.

The string is displaced in a triangular fashion by the plectrum (or the finger-tip, or –nail, or teeth …). After the plucking process, the string moves in a parallelogram-like fashion – given that we take a dispersion-free model as a basis (**Fig. 1.31**). However, this movement in the shape of a parallelogram can only manifest itself if the string does not encounter any obstacles. Frets are potential obstacles; their immediate vicinity has the effect that the string does not only occasionally establish contact but hits them on a regular basis … with the parallelogram-shaped movement being correspondingly changed. **Fig. 1.32** shows (seen from the side) a neck with the typical concave curvature. The axis-relations of this figure hold for the following figures, as well.

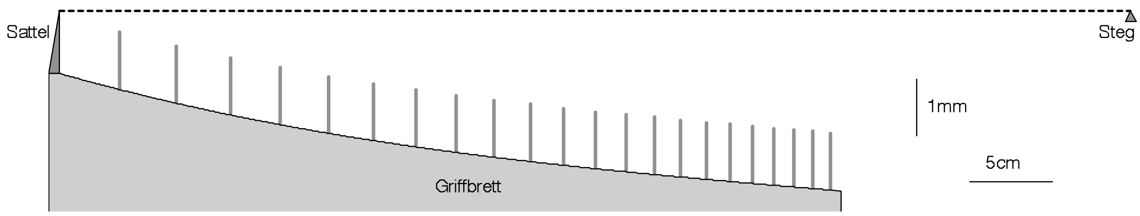

Fig. 1.32: Fretboard geometry (strongly distorted due to the scale); lower surface of the resting string (dashed). The frets are distorted into lines due to the strong magnification of the vertical dimension.
"Sattel" = nut, "Steg" = bridge; "Griffbrett" = fretboard.

If the string pressed down at point A (**Fig. 1.33**) has no contact to the frets, it can freely decay in the dispersion-free model case. The string that has been lifted up, however, hits the 10th fret already after less than half the vibration period – its vibration-shape is completely destroyed.

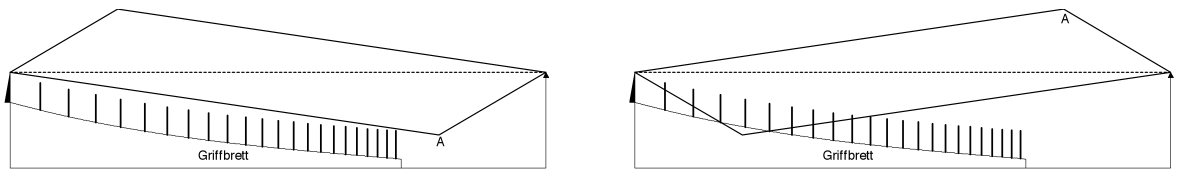

Fig. 1.33: String-parallelogram. On the left, the string was pressed down and then released (uninhibited vibration); on the right it was lifted up and then released (fret-bounce at the 10th fret). “Griffbrett” = fretboard.

The well-versed guitarist will vary his/her “attack” as required and shape the sound of the respective picked note via change of the picking-strength and –direction: both pressing-down and lifting-up of a string happen. However, in particular when using light string sets, a further vibration pattern occurs. It is generated as the string contacts the last fret (towards the bridge) when being pressed down during plucking (**Fig. 1.34**). As soon as the string is released, a transverse wave propagates in both directions and is first reflected at the last fret and then at the bridge. Consequently, a peak running towards the nut is generated – it is reflected there and bounces onto the first fret (right-hand part of the figure).

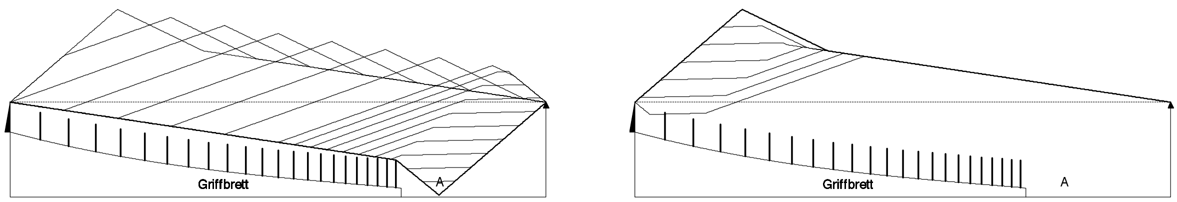

Fig. 1.34: String displacement at different points in time. On the left, the first half-period is shown, on the right we see the subsequent process including bouncing off the first fret. Plucking happens at point A with contact to the fretboard. The time-intervals are chosen such that the resolution is improved at first and after $t = T/2$. Without dispersion. “Griffbrett” = fretboard.

Immediately the question pops up: how often does this case happen? Contact-measurement at the last fret tells us: a lot. For better understanding, **Fig. 1.35** depicts the connection between plucking force (transverse force) and initial string displacement (at A). Since the transverse forces often reach 5 N (or even 10 N occasionally), contact to the last fret often occurs.

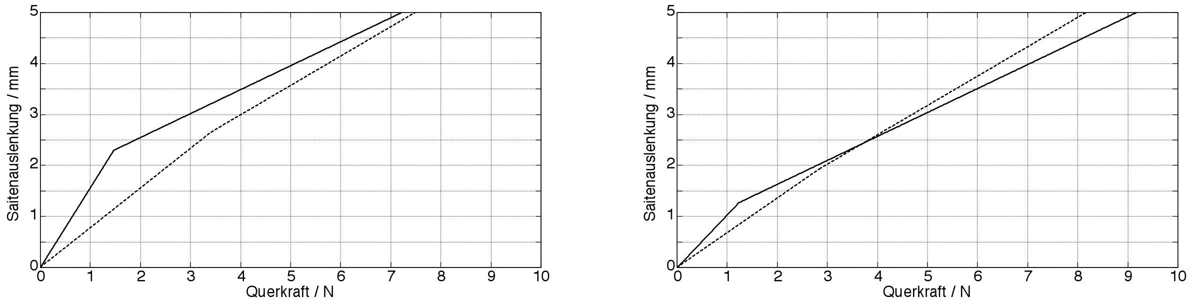

Fig. 1.35: Connection between transverse force and string displacement, open string (left), string fretted at the 14th fret (right), plucking point 14 cm (——) and 6 cm (**---**) from the bridge. 2,1 mm clearance between the string and the last fret (= 22nd fret). B-string, 13 mil, calculations.
“Saitenauslenkung” = string displacement; “Querkraft” = transverse force.

We can see from Fig. 1.35 that the string operates as a linear system only for soft plucking. As soon as the string gets into contact with the last fret, the force/displacement characteristic experiences a knee – a jump in the stiffness of the string occurs. This degressive characteristic tends to correspond to the **behavior of a compressor**: despite stronger plucking force, the string-displacement grows only moderately. However, here we also find a source of potential misunderstanding, for displacement does not equal loudness! With the string establishing contact to the last fret, the shape of the vibration deviates from the mentioned parallelogram, and changes result in the spectrum, and thus in the sound.

For the following graphs, the E_4-string of an **Ovation** guitar (EA-68) was plucked using a plectrum; the electrical voltage of the piezo pickup built into the bridge was analyzed (i.e. the force at the bridge). The location of plucking was at a distance of 125 mm from the bridge, and the plectrum was pressed towards the guitar body such that a fretboard-normal vibration was generated. **Fig. 1.36** shows time function and spectrum for the linear case (no contract between string and last fret). The voltage of the piezo jumps back and forth between 0 V and 0,4 V, with a duty cycle resulting from the division of the string (517:125, scale = 642 mm). Given the transfer coefficient of 0,2 V/N (Chapter 6), the corresponding force at the bridge calculates as 2 N, this representing good correspondence to Fig. 1.35. In this example, 2 N forms the limit of linear operation – using a larger force makes the string bounce off the frets.

This figure is reserved for the print version of this book

This figure is reserved for the print version of this book

Fig. 1.36: Time-function and spectrum of the piezo-signal. The upper half of the left-hand graph shows the measured time function, below is the result of the calculation. On the right is the measured spectrum and the (idealized) envelope. Open E_4-string, fretboard-normal vibration. “Frequenz” = frequency.

The analyses shown in the following graphs (**Fig. 1.37**) correspond to Fig. 1.36 but are based on (fretboard-normal) string excitations of different strengths. For the upper two pairs of graphs we can see proportionality in the time domain and in the spectral domain: the level spectrum is simply shifted upwards for stronger plucking. As soon as the plucking force exceeds 2 N (in the lower two pairs of graphs), the string touches the last fret and bounces off it. Time function and spectrum become irregular. The strong peak in the time function finds its counterpart in the location function (Fig. 1.34); it may be interpreted as the interaction between two excitations:
a) string displacement, force step at $t = 0$ (idealized), and
b) opposite-phase force step at the last fret; occurring at the instant as the string leaves the last fret ($t \approx 0,2$ ms).

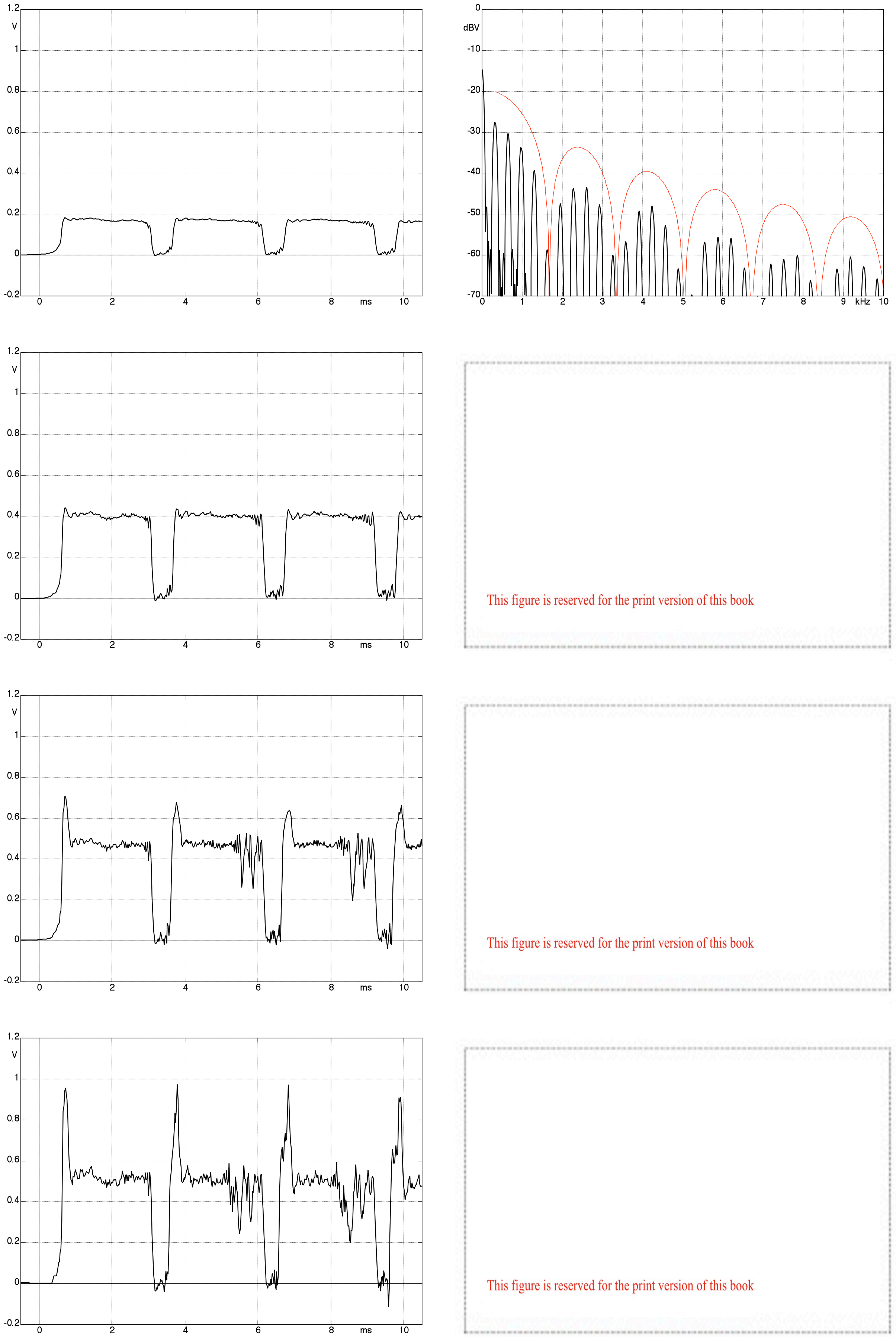

Fig. 1.37: Time-function and spectrum of the piezo-voltage. String plucked with different force. See text.

A spectral analysis encompassing the whole of the auditory range is conducive for the acoustic guitar, and the same holds for a piezo-pickup (Chapter 6). In **Fig. 1.38**, three of the sounds from Fig. 1.37 are shown as third-octave spectra. On the left, we see the spectra of strings plucked lightly and with medium strength, respectively – the system is still linear and the spectra merely experience a parallel shift. Strong plucking (right figure) leads to a level-increase merely in the middle and upper frequency range; below 1 kHz, there is even a decrease in level. As other strings are played, or as the E_4-string is fretted at other frets, this effect tends to remain, but the spectral differences are specific to the individual case.

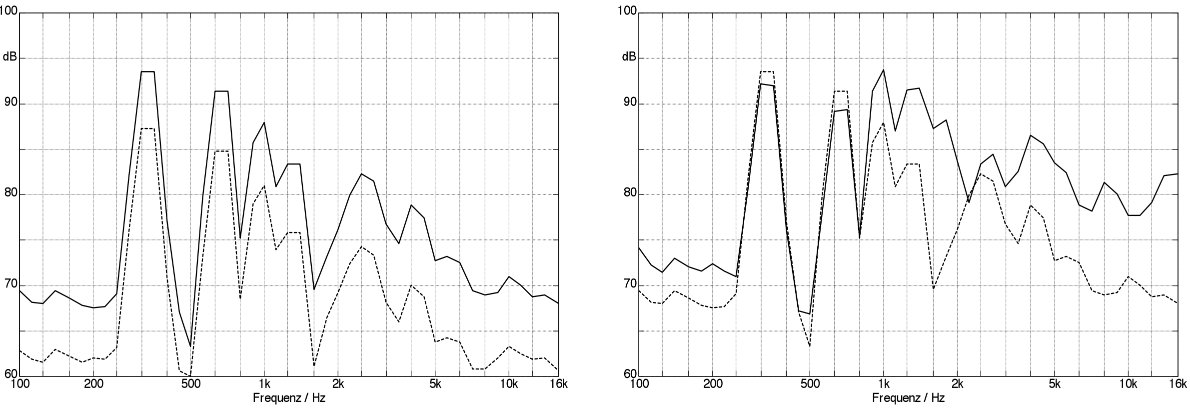

Fig. 1.38: Third-octave spectra, open E_4-string, overlapping analysis of main- and auxiliary third-octave. On the left, and for the dashed curve on the right, there is not yet any bouncing off the frets. Strong plucking (solid line of the right) causes the string to touch the last fret and bounce off it. 1st and 2nd harmonic actually decrease in this process, while there is a strong increase in level at middle and high frequencies.

From this, we can deduce a **compressor-like behavior** in any guitar: for light plucking, the string operates as a linear system, and slight changes in the picking strength lead (with good approximation) to similar level changes in the whole frequency range. However, already at medium picking strength, the string bounces off the frets – the lower the action and the lighter the strings, the lower is the threshold to this occurring. Now, if filtering (due to magnetic pickups) accentuates a specific frequency range, this compression is perceived with different strength. Fender-typical single-coil pickups emphasize the range around 3 – 5 kHz. This will lead to less perception of compression compared to humbuckers sporting resonance frequencies around 2,5 kHz. This may not happen for all played notes, but it does happen in the example shown in Fig. 1.38. So does a humbucker compress more strongly than a single-coil? “Somehow”, yes – but not causally. The source of the compression is the string (in conjunction wit the frets) that compresses in different ways in various frequency ranges. Pickups and amplifiers make this different compression audible in different ways.

Here’s an opinion voiced in the Gitarre & Bass magazine (02/2000): "What happens when I, for example, pick the low E-string first softly and then more and more strongly via a slightly distorted amp? The Strat behaves much more dynamically and you can open the throttle ever more until, purely theoretically, the string throws in the towel and breaks. The Les Paul shows an entirely different character: first, the increasingly harder picking also generates more loudness, but then the whole thing topples over: the notes don’t get louder anymore but more dense – almost as if there were a compressor/limiter switched in. Say what?! Indeed, the information of the string vibrations resulting from the behavior of the wood determines the tonal characteristic of the Les Paul, but not the fatter sounding humbuckers.”

The G&B-author was careful (?) enough not to throw in something like "and that shows that mahogany compresses more strongly than alder". Still, he infers: "*now we understand, why a Strat even with Humbuckers can never turn into a Les Paul. You can at most make the tone warmer and fatter, but the typical compression is out of reach.*" Unfortunately, the author does not report which experiments or models were the basis for his last conjecture.

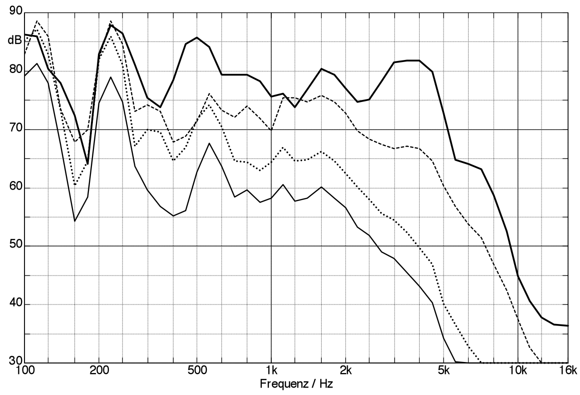

Fig. 1.39: Third-octave spectrum, Stratocaster, neck-pickup, E_2-string (42mil) fretted at the 5th fret. Plucked from lightly to strongly. Distance between plectrum and bridge: 13 cm. Clearance of the open E_2-string to the last fret: 2,3 mm.

As we can see from **Fig. 1.39**, a **Stratocaster**, too, compresses in the range of the low partials. While the level-difference between light and very strong plucking is no less than 39 dB at 4 kHz, the fundamental changes only by 7 dB. Your typical Gibson Humbucker will only transmit the spectrum of the low E-string up to about 2 kHz and therefore misses the dynamic happening in the 4-kHz-range that a Fender pickup will still capture. However, in the experiment reported in G&B, it is likely that behavior of the amplifiers was almost more important: *"via a slightly distorted amp"*. There you go! The Gibson Humbucker will have generated approximately double the voltage of the Fender single-coil. That makes the **amplifier** participate in the signal compression: it will compress (or limit) the louder signal (that of the Les Paul).

However, that does not mean that the compression is determined merely by the action on the guitar, and by the amplifier. As the string bounces off the fret, a metal hits metal (at least on the electric guitar). The result is a broad-band bouncing noise that extends to the upper limit of the audible frequency range. String- and fret-materials are of particular significance in this bouncing noise: pure-steel wound strings generate a more aggressive, treble-laden noise compared to pure-nickel wound strings. Old string with their winding filled up by rust, grease, etc, will sound duller than fresh strings. And the **fret-wire** that the string hits (that may in fact be any fret in the course of the vibration) contributes, with its mechanical impedance, to the bouncing noise, as well. A detailed analysis of the mechanical neck- and body- impedances follows in Chapter 7; string/fret-contacts are analyzed in detail in Chapter 7.12.2.

1.5.4 String-buzz

If the string is plucked with little force, it reacts approximately as a linear system. This implies that double the initial displacement also leads to double the displacement at every moment during the subsequent vibration process. Of course, the displacement cannot become indefinitely large – at some point the string will hit the frets on the neck (Chapter 1.5.3, Chapter 7.12.2). If this contact to the fretboard happens right after the plucking itself, it becomes part of the attack process of the respective tone. Later occurring contacts to the frets (with the limit at later than about 50 ms) will become audible as single events – given they are strong enough. Weak or short string/fret contacts are, to some degree, a means of expression and therefore not generally undesirable.

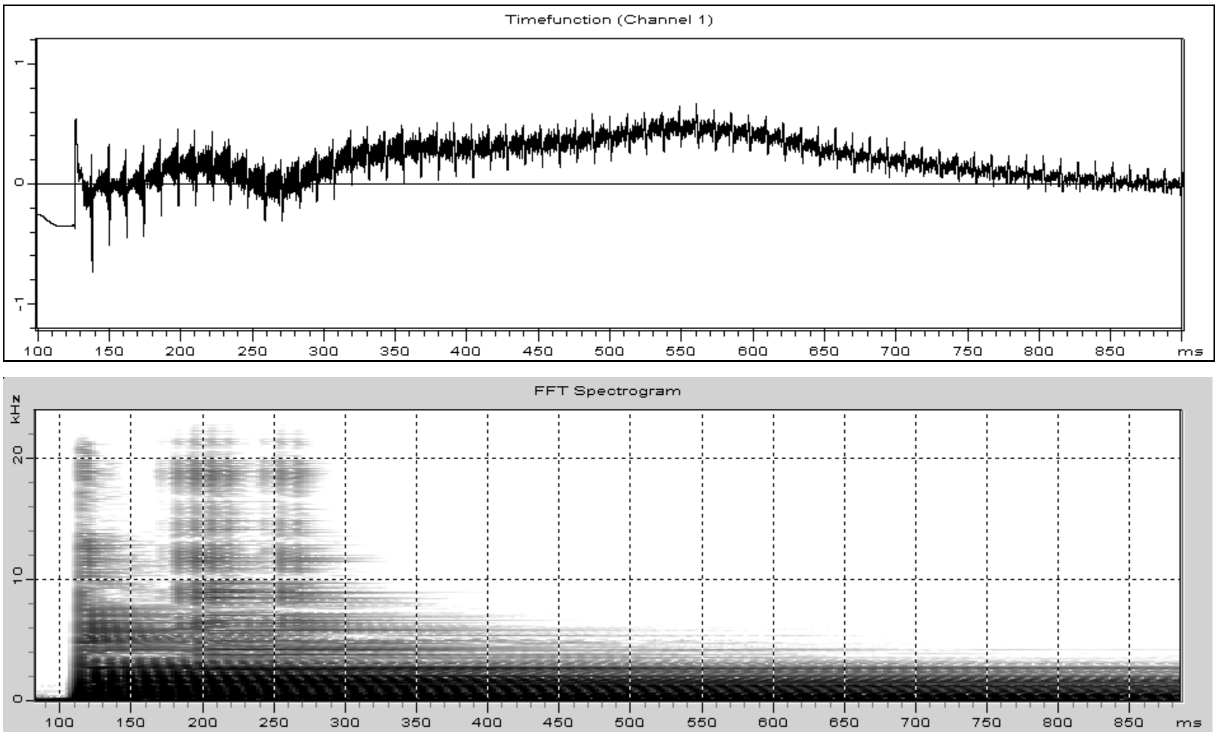

Fig. 1.40: Time-function and spectrogram of the piezo voltage resulting from a strongly plucked low E-string (E_2).

In **Fig. 1.40** we see the piezo voltage taken from an OVATION Adamas SMT (open E_2-string), with the string so strongly plucked with a plectrum that a clear buzz became audible. The spectrogram reveals – after the broadband first plucking impulse has passed – further string-to-fret hits around 200 and 350 ms; these act like high-frequency echoes. The string hits the frets repeatedly and strongly, and generates a clearly audible buzz.

Besides the impulses occurring with a separation of 12 ms, very low-frequency vibrations are visible in the time-function. These point to the reason why the string bounces off the fret not only at the very beginning of the vibration. However, an exact analysis of the low-frequency vibration cannot be derived from the time-function. This is because the cutoff-frequencies found in the piezo pickup, the amplifier and the analyzer at around 2 Hz result in strong phase shifts. The cause of the low-frequency signal components is a rotation of the plane of vibration (Chapter 7.7.4, Chapter 7.12.1).

1.6 The decay process

After being plucked, the sting vibrates in a free, damped oscillation process. “Free” implies that no further energy is injected; “damped” indicates that vibration energy is converted into sound and caloric energy (radiation, dissipation). Any further string damping (e.g. via the fingertips of the palm of the hand) shall not be considered here at this time.

1.6.1 One single degree of freedom (plane polarization)

The simplest oscillation system consists of a mass, a spring, and a damper. The mass force is proportional to the acceleration (inertia, NEWTON), the spring force is proportional to the displacement (stiffness, HOOKE), and the damper force is proportional to the (particle) velocity (friction, STOKES). The time derivative of the displacement yields the velocity; the time derivative of the velocity yields the acceleration [3].

After the excitation a “periodic” oscillation of the frequency f_d results. Instants of equal phase (e.g. maxima, zeroes, and minima) occur at equal distances in time – which led to the us of the term **period** $T = 1/f_d$. However, signal theory does not actually see this decay process as a periodic signal: due to the exponential decay, the individual periods fail to be identical. Mechanics, on the other had, do use the term periodic vibration here because the duration of the periods in time-invariant (... non est disputandum).

The resulting envelope has three parameters: the frequency f_d, the initial phase φ, and the time constant of the envelope ϑ. In this general form, the equation for the oscillation is:

$$\xi(t) = \hat{\xi} \cdot e^{-t/\vartheta} \cdot \sin(2\pi f_d t + \varphi), \qquad t \geq 0 \qquad \text{Oscillation equation}$$

For $t = 0$, the e-function yields 1; with increasing time, it decreases towards 0. The phase shift φ may be taken to be zero for the first considerations. The time constant ϑ determines how fast the oscillation decays: the smaller ϑ is, the faster the decay. Instead of ϑ, literature offers a multitude of other parameters, as well – they can easily be converted into each other. The letter τ is frequently used for the time-constant; in the present context we will rely on this letter only when we get to the calculation of levels. What needs to be avoided in particular is confusion between the degree of damping and the decay-coefficient, since the latter is sometimes also designated with ϑ!

It may be the displacement, the (particle) velocity, or the acceleration that represents the physical oscillation. A sensor converts these quantities into a voltage $u(t)$ that subsequently is analyzed.

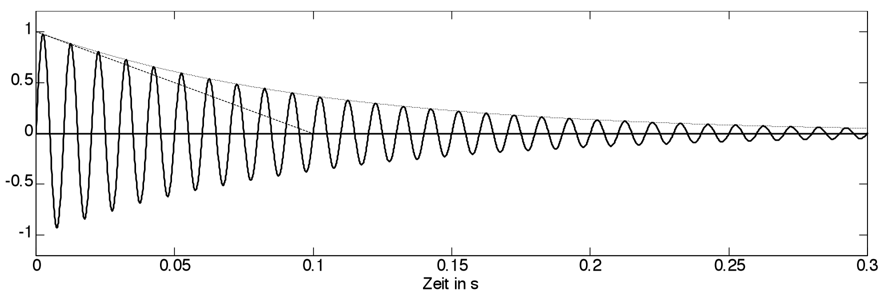

$$f_d = 100\,\text{Hz}$$

$$\vartheta = 0{,}1\,\text{s}$$

Fig. 1.41: Damped oscillation of 100 Hz; exponential decay; time-constant $\vartheta = 0{,}1\,\text{s}$.

Given mass m, spring-stiffness s, and friction W, we calculate frequency and time-constant:

$$f_d = \frac{1}{2\pi}\sqrt{\frac{s}{m} - \frac{1}{\vartheta^2}} \qquad \vartheta = \frac{2m}{W}$$ Parameters of the oscillation

If the friction W is set to zero, the un-damped system results. It has an infinite time-constant: the e-function now has the constant value 1, and the vibration does not decay anymore. A weakly damped vibration with a frequency $f_d = 100$ is shown in **Fig. 1.41**. The shape of the e-function is indicated as a dashed line with its tangent crossing zero at ϑ. At the point in time of $t = \vartheta$, the envelope has decreased from 1 to $1/e \approx 0{,}37$.

In instrumentation, the decay process is often depicted as **level-curve**. Level is a logarithmic measure that may be determined in various ways. It always constitutes a time-average over a weighted measurement interval; the averaging is done using the squared signal quantity. We often see an exponential averaging where the weighting is of exponential form, and is done such that the signal components lying further back in the past contribute less prominently to the measurement. The **averaging time constant** $\boldsymbol{\tau}$ is specified as parameter of the exponential averaging; the value $\tau = 125\,\text{ms}$ is used frequently, with the corresponding standardized way of averaging being labeled **FAST**. The decay constant ϑ of the dampened oscillation must not be confused with the averaging time constant τ of the level measurement.

The level measurement comprises three consecutive operations: squaring, averaging, and logarithmizing. Squaring and logarithmizing are non-linear operations; the order of sequence must therefore not be interchanged. It is only the averaging that is a linear filter operation: a 1st-order low-pass in the case of the level measurement. In the time domain, the averaging is described by a convolution [6]: the result of the averaging corresponds to the convolution of squared signal and impulse response $h(t)$ of the averager. For damped oscillations we get:

$$m(t) = h(t) * u^2(t) = \int_0^t \left(\frac{1}{\tau} e^{\frac{\psi - t}{\tau}}\right) \cdot \left(\hat{u} \cdot e^{-\psi/\vartheta} \cdot \sin(\omega_d \psi)\right)^2 \cdot d\psi$$ (for causal signals)

$$h(t) = \frac{1}{\tau} e^{-t/\tau} \qquad u(t) = \hat{u} \cdot e^{-t/\vartheta} \cdot \sin(\omega_d t) \qquad \omega_d = 2\pi f_d$$

Here, $h(t)$ is the impulse response of the averager, $u(t)$ is the damped oscillation, the star symbol stands for the convolution. The average $m(t)$ is calculated for the point in time t with the time-variable ψ integrated from 0 to t. Therefore, the **average value** $m(t)$ does in this case not indicate the average over the whole decaying oscillation but the average from the excitation to the (variable) point in time t. The averaging time constant τ is large compared to the oscillation period T; the contribution of the sine function can thus be disregarded in good approximation. Using this, the time-variant average is:

$$m(t) = \frac{\tilde{u}^2}{1 - 2\tau/\vartheta} \cdot \left(e^{\frac{-2t}{\vartheta}} - e^{\frac{-t}{\tau}}\right) \qquad \tilde{u} = \hat{u}/\sqrt{2} \qquad \text{for } 2\tau \neq \vartheta$$

When calculating levels we need to consider that we are working with a squared signal, which is why we need to opt for the formula for power levels. The reference value needs to be chosen such that the correct absolute value results for the steady case ($\vartheta \to \infty$). Using, on the other hand, $u_0 = \tilde{u}$, we get the relative level that decays starting from 0 dB.

$$L(t) = 10\lg\left(m(t)/u_0^2\right)\text{dB} \qquad \text{dB} = \text{decibel} \qquad u_0 = \text{reference value}$$

Fig. 1.42 shows the course of the level of a damped oscillation determined via exponential averaging. The time-constant of the damping is $\vartheta = 4\,\text{s}$. Having an understanding of the equation of the oscillation, we could also give the exact course of the level. To do that, it is merely necessary to logarithmize the *e*-function (shown as a dashed line). The level determined via measurements deviates significantly from this calculation. In the figure, we see two graphs with the averaging time-constants 0,125 s and 0,5 s, as well as the theoretical behavior (dashed).

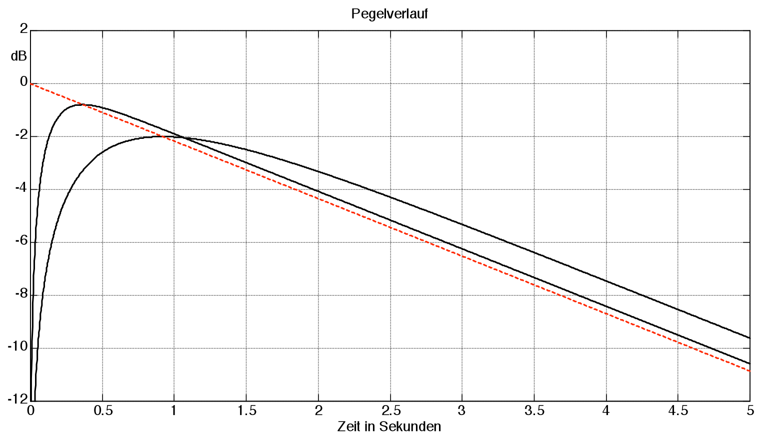

Fig. 1.42: Level of an exponentially damped oscillation. Damping time-constant ϑ = 4 s, averaging time constanr, τ = 125 ms and 500 ms. For 500 ms, the asymptote is too high by 1,2 dB, and for 125 ms, it is too high by 0,3 dB.
"Pegelverlauf" = course of the level; "Zeit in Sekunden" = time in seconds

After a short attack phase (mainly determined by τ), the level drops off with approximately the time constant ϑ. As is evident, the measurement curves run in parallel to the exact values after a short time, but remain too high. Therefore the slope – and thus the system damping – can be determined with good accuracy; for measurements of absolute values, however, considerable errors may arise. Using $L(t)$, the level difference is calculated as:

$$\Delta L = 10\lg\frac{1}{1 - 2\tau/\vartheta}\text{dB} \qquad\qquad \left.\vartheta = 10\tau \;\right\}\; \Delta L \approx 1\text{dB}$$

The shorter the averaging time-constant gets relative to the damping time-constant, the more exact the tracing of levels via measurements becomes. Still, the averaging time-constant must not be chosen too short, either, because then the (squared) oscillation may not be fully averaged anymore, and ripples in the level-graphs would result.

Moreover, Fig. 1.42 indicates that the measured **level maximum** is lower than expected. The position of the maximum is determined via differentiating and zeroing:

$$t_{\max} = \frac{\ln(2\tau/\vartheta)}{2/\tau - 1/\tau} \qquad\qquad m_{\max} = \tilde{u}^2 \cdot \left(\frac{\vartheta}{2\tau}\right)^{\frac{1}{1-\vartheta/2\tau}}$$

The larger the averaging time-constant is chosen, the lower the maximum.

From a signal-theory point-of-view, a damped oscillation belongs with **energy signals**. The signal energy is derived as integral over the squared signal value; it differs from the physical energy:

$$E_{Signal} = \int_{-\infty}^{\infty} u^2(t)\,dt \qquad E_{phys} = \int_{-\infty}^{\infty} F(t)v(t)dt = \int_{-\infty}^{\infty} v^2(t)\cdot Z\cdot dt \qquad Z = \text{impedance}$$

The signal energy of the damped oscillation may be calculated from the equation of the oscillation using integration:

$$E = \int_{0}^{\infty} \left(\hat{u}\cdot e^{-t/\vartheta}\cdot \sin(2?f_d t)\right)^2 dt \xrightarrow{\vartheta\cdot f_d \;>>1} E = \hat{u}^2\cdot \vartheta/4$$

The average value across $m(t)$ yields the same signal energy irrespective of τ. If the energy is derived via $m_{\max}$, however, a correction is required due to $m_{\max} < \tilde{u}^2$.

Besides the exponential averaging there are also other ways to average: block-averaging is done with constant weighting across a fixed time interval, Hanning-averaging uses a sine-shaped weighting. Block averaging is also called **linear averaging**, a rather confusing term that is common in the area of spectral analysis, though. While the exponential averaging is always run from the start of the signal to the point in time of the measurement (marked with a star on Fig. **1.43**), linear averaging is done from the start of the signal over an interval of fixed duration (1 s in the figure). In exponential averaging, only the end of the interval is shifted, in linear averaging, however, this is done to both start and end. **The Hanning-averaging** uses a fixed duration of the averaging (2 s in the figure), as well, but weighs the signal with a $\sin^2$. Hanning-averaging is often deployed in DFT-analyzers – as are many other DFT-windows (Blackman Kaiser, Bessel Gauß, Flat-Top, etc.).

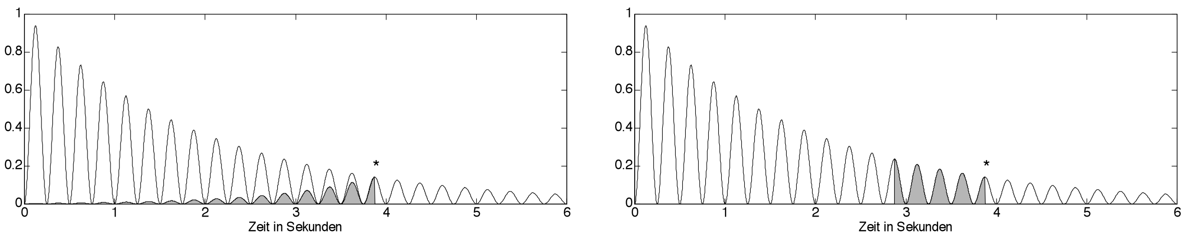

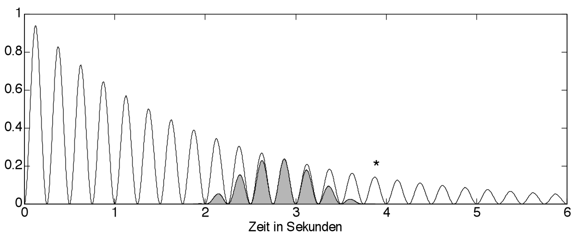

Fig. 1.43: Different ways of averaging: exponential averaging (upper left), linear averaging (upper right), Hanning-averaging (lower left).
"Zeit in Sekunden" = time in seconds"

All ways of averaging are calibrated such that for steady signals (constant level), equal results are obtained. With levels varying over time, differences occur. In frequency-selective analyses (DFT, 1/3rd-octave, etc.), also further system-immanent errors contribute: a filter will react more sluggishly to the input signal as the filter band becomes narrower. In broadband level-measurements (e.g. 10 Hz – 20 kHz), no significant errors will occur, but in selective measurements of partials (e.g. 2500 Hz – 2519 Hz), they might creep in, depending on circumstances.

1.6.2 Spatial string vibrations

After a guitar string is plucked, spatial vibrations will propagate on it. The transversal waves introduced in Chapter 1.1 are of particular significance. Given that the axis along the string is taken as z-coordinate, transversal waves can propagate both in the xz-plane and the yz-plane; superpositions are possible, as well. For electric guitars, the vibration plane perpendicular to the guitar top is especially important, while for acoustic guitars the vibration parallel to the guitar top also has effects.

The wave equation includes a dependency both on place and time. However, investigations into the vibrations of guitar strings are mostly based on a fixed location (the place of e.g. pickup, or bridge) so that merely the time remains as variable. As a simplification, the string vibration occurring at a given location tends to be seen as superposition of many exponentially decaying partials (Chapter 1.6.3). In this scenario we need to consider, though, that for each partial, vibrations may appear in two planes. Sometimes one of the two vibrations has next to no effect and may be disregarded, but in some cases both need to be taken into consideration.

The following approaches first start from the assumption that plucking the string will result in two *same-frequency* vibrations orthogonal in space. The time constants of the damping ϑ are still different for the two vibrations, the effect on the output is different, and they may be phase-shifted relative to each other. At the output, both are superimposed:

$$u(t) = \hat{u} \cdot \left(e^{-t/\vartheta_1} \cdot \sin(\omega t) + d \cdot e^{-t/\vartheta_2} \cdot \sin(\omega t + \varphi) \right) \qquad d = \text{top-parallel part}$$

Particularly in acoustic guitars, the top-normal vibration is tightly coupled to the resulting sound field, and therefore vibration energy is relatively quickly withdrawn, and the damping time-constant is short. The top-parallel vibration does not lead to as efficient a radiation (d is smaller); it thus has a longer time-constant. In the level-analysis, the decay shows up with a characteristic kink (**Fig. 1.44**).

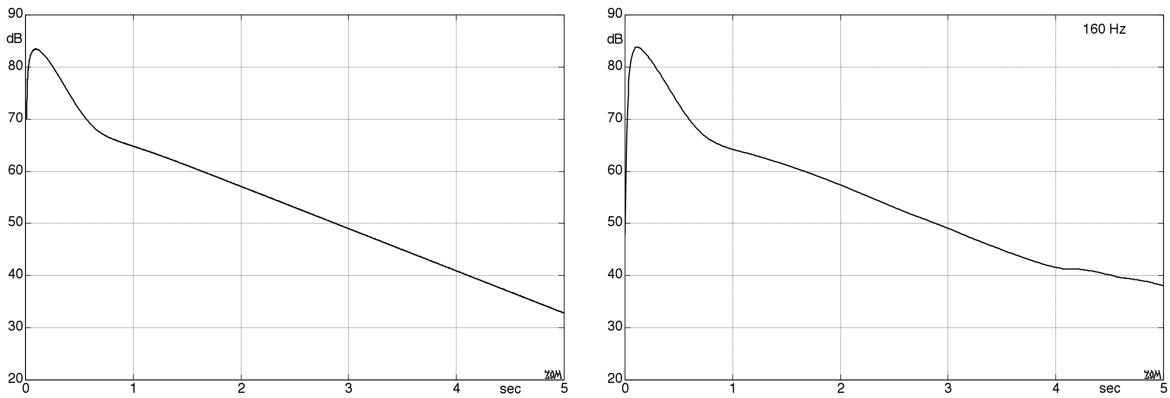

Fig. 1.44: Open E_2-string, FAST-level of the 2nd partial; *left*: calculation; *right*: measurement (Martin D45V).

To confirm our hypotheses about the vibrations, two experiments were carried out. In order to adjust the neck, the OVATION Adamas SMT allows for the removal of a cover plate (of ∅13cm) in the guitar body. This detunes the Helmholtz resonance and thus changes the low-frequency coupling to the sound field. With the cover taken off, the low frequencies receive weaker radiation; the time constant should therefore be longer.

This figure is reserved for the print version of this book

This figure is reserved for the print version of this book

Fig. 1.45: Left: Ovation Adamas SMT, level of fundamental (F#$_2$), with closed ("Deckel geschlossen") and removed ("Deckel geöffnet") cover plate.
Right: Ovation Viper EA-68, level of fundamental (F#$_2$), with ("mit Magnetfeld") and without influence of the magnetic field.

Fig. 1.45 (left) depicts the decay curves for the fundamental of the tone F# fretted at the 2nd fret on the low E-string. The measurements confirm the assumption. In a second experiment, a **permanent magnet** was brought close to the low E-string on an OVATION Viper. Due to the attraction force the stiffness of the string is reduced in *one* plane of vibration – the vibration frequency is thus reduced in that plane. This leads to a **beating** of the orthogonal fundamentals now slightly detuned relative to each other (**Fig. 1.45**, right).

However, even without any magnetic field, the top-normal vibration of a particular partial does not necessarily occur at the exact same frequency as that of the top-parallel vibration of the same partial. This is due to the reflection factors of the string clamping (nut, bridge) – the former are dependent on the vibration direction. The spring-stiffnesses at the edges may be different for the two directions of the vibration, resulting in slight differences in the vibration frequencies. The decay process will then include beatings that render the sound more "lively". **Fig. 1.46** shows results of calculations and, for comparison, sound pressure levels measured with an acoustic guitar (MARTIN D45V, anechoic room, microphone at 1 m distance ahead of the guitar). Various patterns emerge:

The level differences between the two sub-vibrations determine the *strength* of the interference. At a difference of 20 dB, the amplitude fluctuates merely by 10%, while at 6 dB difference the fluctuations grow to 50%. Differences in the damping determine for which *period* the beating persists. If both sub-vibrations decay with the same damping, the level-difference does not change, and neither does the beat-intensity. Conversely, if the decay is different, the beats are strongest at the instant when both levels are equal. The frequency difference determines the *periodicity in the envelope*: the larger this difference, the faster the fluctuations. Moreover, the *phase* of the sub-vibrations is of significance – in particular if different damping occurs i.e. if the beats are limited to a short time-interval. The interference-caused cancellation will only present itself if both sub-vibrations are in opposite phase during said time-interval.

Another degree of freedom comes into play if we allow for **non-linearities**. For example, the friction may depend on a higher order of particle velocity, or the spring-stiffness may depend on the displacement. This may cause, for example, that the level of a mono-frequent vibration does not decay linearly with time but shows a curvature. Addressing such aspects requires considerable effort – no corresponding investigations were carried out in the present framework.

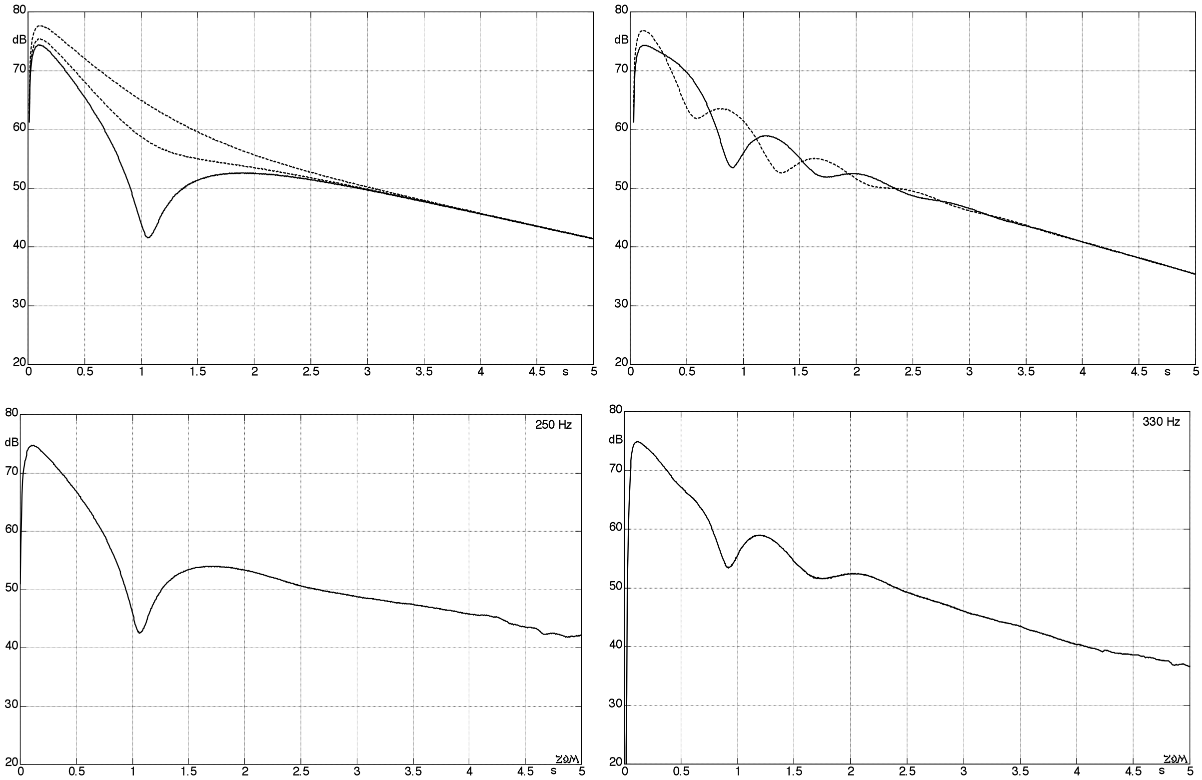

Fig. 1.46 Top: Decay processes given phase-differences. Left: both vibrations with the same frequency; right: beats due to a frequency differencde of 1.2 Hz. The damping cannot be determined precisely anymore from the initial slope of the curve. **Bottom**: measurements with a MARTIN D45V

An interesting set of curves emerges if the excitation energy remains constant while the string damping varies. First, however, we need to define more precisely the term “damping”: any real string executes a damped vibration. In this case, **damping** means that vibration energy is continuously withdrawn from the string, with displacement amplitude (potential energy) and velocity amplitude (kinetic energy) decreasing over the course of time. Springs and masses store energy while resistances “remove” energy. Sure, energy cannot actually be removed – rather its mechanic incarnations are converted into caloric energy (heat); but in any case the “removed” energy is not available anymore to the vibration of the string.

In the **acoustic guitar**, we need to distinguish between the ‘good’ and the ‘bad’ losses. If all of the energy in the string is converted to sound-energy with an efficiency of 100%, we do have damping (a loss), but the objective of generating sound has been achieved with the utmost efficiency. If, conversely, 90% of the energy in the strings is converted directly into heat due to inner friction, and only 10% are radiated, we have an undesirable loss. To illustrate this with an EXAMPLE: a watering can supplies water to a flowerpot. If the water flows through a small cross-section, it will take a long time until the can is empty. With a larger cross-section, the process will be quicker – but it’s always the whole of the water that arrived in the flowerpot. This situation changes if there is a hole in the bottom of the can – an additional degree of freedom is now present that influences the efficiency ◊. Applying this to the string: via tight coupling between string and sound field, the energy flows from the string quickly – the string is damped strongly but all energy reaches the sound field (100% efficiency). The efficiency drops only as friction-resistance is included in the guitar.

In **electric guitars**, the objective is entirely different. They do not need to radiate sound energy – that's taken care of by the loudspeaker. Due to the lack of radiation loss, the string damping is lower, the decay is longer – the guitar has longer/better **sustain**.

Several quantities are disposable in order to describe damping: one is the time constant of the damping (or **time constant of the envelope**) ϑ of the individual partials. During the length of a time constant, the level of the respective partial drops by 8,686 dB. A vibration with a level dropping off by 60 db within 10 s has a time constant of 1,45 s. The duration of time that it takes a level to drop by 60 dB is – in room acoustics – also called the **reverberation time T_N**. The latter is suitable to describe a damping, as well: the formula $T_N = 6{,}91 \cdot \vartheta$ holds. **Fig. 1.47** shows the course of the levels of the fundamentals (*G#*) measured via the piezo pickup. During the initial second, the time constants differ by a factor of 18.

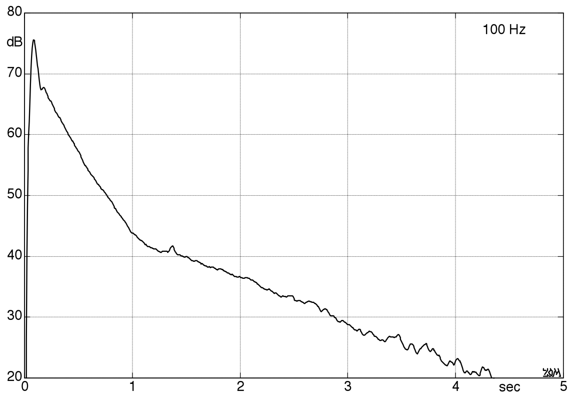

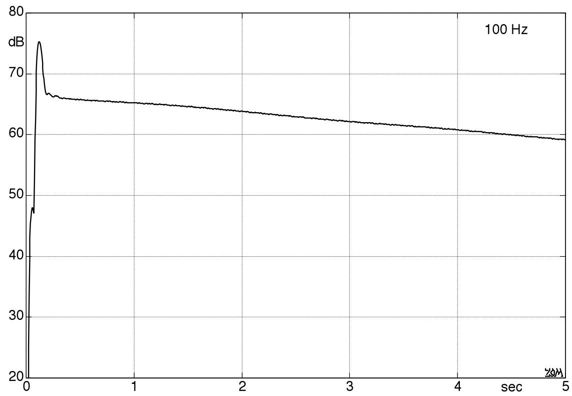

Fig. 1.47: Measurements with Ovation guitars: SMT (acoustic guitar, left); Viper (electric guitar, right).

The following considerations are based on the law of conservation of energy. In the plucking process, the string is given a certain potential energy that is in part dissipated and in part radiated. As an EXAMPLE, a string is to be plucked with 5 mWs; it then decays in different ways. Which sound pressure level is generated at a distance of 1 m if we assume – to begin with – that 100% of the vibration energy is radiated as **sound wave**?

For any exact calculation we would have to know about the beaming – as a simplification let us assume an omni-directional characteristic here. In fact, this assumption is a good approximation for the (quite level-strong) 2nd partial of the E-string [1]. The energy E of the spherical wave [3] is calculated as:

$$E = \frac{4\pi R^2}{Z_0} \int_0^\infty p^2(t)dt = \frac{4\pi R^2}{Z_0} \cdot \frac{\hat{p}^2}{4} \cdot \vartheta \qquad \text{with } Z_0 = 414 \text{ Ns/m}^3$$

Herein, $p(t)$ is the sound pressure at the distance R = 1m; the integral over the damped vibration was already calculated at the end of Chapter 1.6.1. The equation can be solved for the sound pressure amplitude:

$$\hat{p} = \sqrt{\frac{Z_0}{\pi R^2} \cdot \frac{E}{\vartheta}} \quad \text{in the example} \quad \hat{p} = 0{,}57\,\text{Pa} \quad \text{for } \eta = 100\% \text{ und } \vartheta = 2\,\text{s}.$$

From the (now known) sound pressure, the level can be calculated e.g. for exponential FAST-averaging (**Fig. 1.48, left section**, different ϑ). ◊

$$L(t) = 10\lg\left(\frac{Z_0 E/p_0}{2\pi R^2(\vartheta - 2\tau)} \cdot \left(e^{-2t/\vartheta} - e^{-t/\tau}\right)\right) \qquad \vartheta \neq 2\tau$$

The time constant ϑ of the damping influences both the maximum value and the speed of decay. The luthier can increase the peak sound pressure level via high mechano-acoustical coupling – the loudness will then decrease more quickly, though. Lower coupling will enable him (or her) to achieve longer sustain, but then the guitars is not as loud. The plucking energy is present only once, after all. Now, if we allow the string to vibrate in two planes, the seemingly impossible is in reach: a loud guitar with long sustain. The top-normal vibration generates a loud attack. The quick decay of this loud attack is “drowned out” after a short time by the more slowly decaying top-parallel vibration.

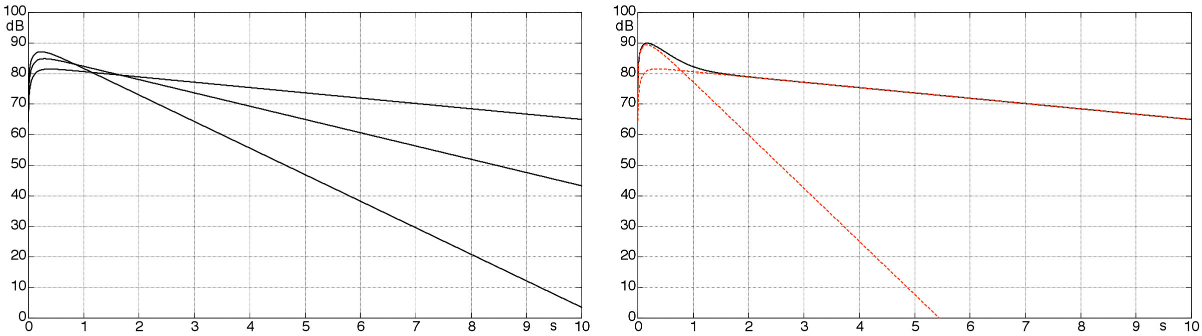

Fig. 1.48: Left: FAST SPL for different degrees of coupling between string and sound field (η = 100%). Right: FAST-SPL for two superimposed orthogonal vibrations (η = 100%). Equal energy.

Fig. 1.48 (right hand section) shows an example with both vibrations being excited with 5 mWs. The quicker decay happens at a time constant of the damping of 0,5 s, the longer decay has a time constant of 5 s. The dashed lines indicated the levels of the individual vibrations. An efficiency of 100% is assumed again for both vibrations.

Of course, in practice an **efficiency** of 100% is not achievable; part of the vibration is converted into caloric energy already within the string, and in the guitar body, as well. Reducing the efficiency to 50% will also reduce the time constant of the decay by half (this may be deduced via the transmission-line equation). The course of the level will then be determined by two parameters: the mechano-acoustical matching, and the dissipation in the guitar (**Abb. 1.49**).

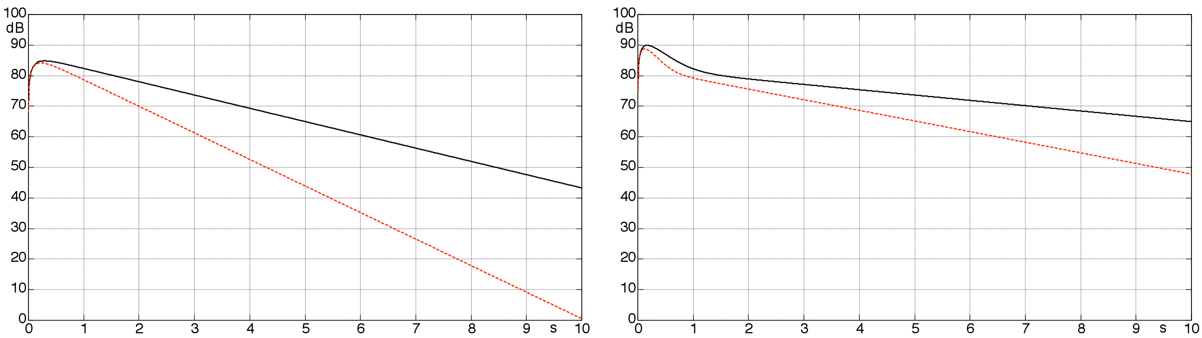

Fig. 1.49: Calculated SPL for an excitation energy of 5 mWs (left) and 2.5 mWs (right). The solid line indicates an efficiency of 100 %, the dashed one an efficiency of 50%.

1.6.3 Partial and summation-levels

The real guitar string does not consist of a single concentrated mass and a single concentrated stiffness – rather, these quantities are continuously distributed along the length of the string. As a consequence of this spatial distribution, a multitude of Eigen-vibrations (natural vibrations) manifest themselves (Chapters 1.1. and 1.3), all of which decay with their individual frequency f_i, initial phase φ_i and damping ϑ_i. The actual overall vibration is a superposition (addition) of the individual vibrations that also appear in two planes each – again with different parameters. This already rather complex description is, however, still a simplification because we would have to consider non-linear behavior in addition, especially for strong plucking.

Typically, low-frequency partials show long sustain while high-frequency partials decay quickly – especially with old strings. The course of the levels of individual partials needs to be determined frequency-selectively, e.g. using a narrow band-pass filter with its center-frequency tuned to the frequency of the given partial. Choosing a filter bandwidth that is too wide will make the neighboring partial influence the measuring result; with too narrow a bandwidth, fast changes in level will not be captured correctly. From a systems-theory point-of-view, two filters are connected in series: the string and the band-pass. The output signal results from the filter input-signal (string vibration) convolved with the impulse response of the band-pass filter. The narrower the band of the filter, the slower its impulse response decays, and the less the course of the level of the partial is correctly captured.

This is an inherent problem existing irrespective of how the narrow-band filtering is achieved. A DFT (Direct Fourier Transform) can be interpreted as a filter-band: for this the DFT-window (e.g. Hanning) is moved along the time axis, and the now time-variant voltage of each discrete frequency point is interpreted as time-discrete output voltage of the filter (STFT = short-time Fourier Transform).

In the STFT, the time signal $\underline{u}(t)$ to be analyzed is first multiplied with a weighing window; this weighing function is different from zero only for a short time. The DFT is calculated across the signal weighted this way, resulting in a complex instantaneous value at the individual frequency *f*. Then, the window is shifted by one sample period, und again a DFT is calculated … and so on.

$$\underline{U}(t',\omega) = \int_{-\infty}^{\infty} \underline{u}(t)\cdot g(t'-t)\cdot e^{-j\omega(t'-t)}\cdot dt \qquad \text{STFT}$$

$$\underline{z}(t') \quad = \int_{-\infty}^{\infty} \underline{x}(t)\cdot \underline{y}(t'-t)\cdot dt \qquad \text{Convolution}$$

Formally, the integration for the STFT happens across the infinitely lasting time *t*. De facto, however, this is done merely across the window-section that is shifted by *t'*; the *e*-function is due to the Fourier transform. The convolution integral has the same structure – its first factor is seen as time function to be filtered. Its second factor results – as impulse response – in a vibration of the circular frequency ω that is weighted with $g(t)$. This shows that the STFT works like a (digital) filter – including all associated system-typical selectivity-problems.

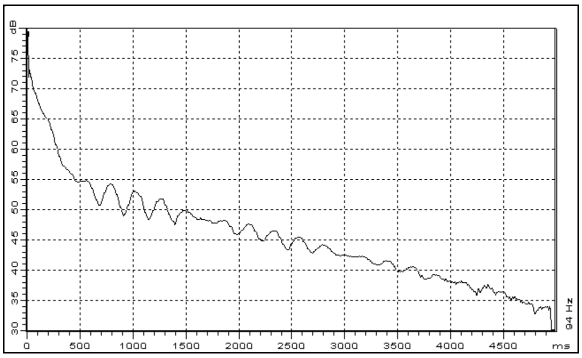

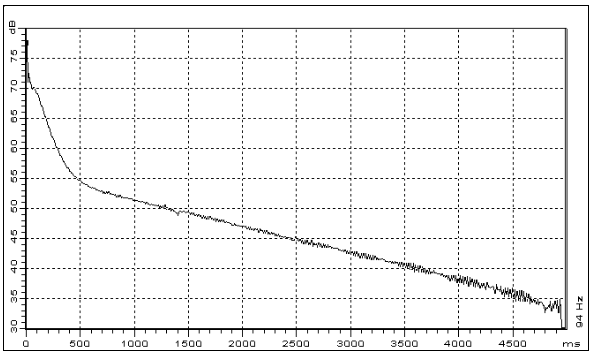

Fig. 1.50 Course of the level of the fundamental (*G#*): 40-dB-Kaiser-Bessel-window (left), 60-dB-Kaiser-Bessel-window (right).

While merely *one single* (theoretical) long-term spectrum exists, there are any numbers of short-term spectra that in some cases differ substantially. In **Fig. 1.50**, the same decay process is investigated using two different DFT-windows. The beats visible in the left-hand section of the figure are leakage effects of the DFT-window, as they would appear similarly also with the Hamming window and the 40-dB-Gauss-window♣. Although this analysis could not be actually termed ‘wrong’, it is more purposeful to use a window with stronger side-lobe attenuation (e.g. 60 dB; right hand section of the figure).

A 512-point DFT at 48 kHz sampling rate will have a frequency-line distance of 94 Hz. This frequency grid is too coarse to obtain a good resolution of an E2-spectrum (fundamental frequency 82,4 Hz). Using an 8k-DFT reduces the line distance to 5.9 Hz; however, at the same time the block length rises to 171 ms. Basis of the selective level measurement is now an averaging time of 171 ms (due to the filter, with a weighting corresponding to *g(t)*), and this smoothes out all quick changes in level. A compromise needs to be found between these two extremes.

The overall level can be calculated via summation of the temporal course of the partial-levels. However, this does not work by simply adding the dB-values; rather, it is necessary to add the individual *power* data (addition of incoherent sources). Since power is always positive, the overall level can never be smaller than the individual levels – if the latter are all measured using the same type of averaging, that is! Given different averaging, the value of the sum can indeed have a short-term value smaller than the individual values.

In summary, the following picture emerges: the *power* of the partials decays (in approximation) exponentially while the *level* of the partials decreases linearly. If the fretboard-normal and the fretboard-parallel components of the vibration show different damping, a kink can appear in the course of the level. If moreover the frequencies are also different, beats can result. Averaging techniques that are unavoidable when taking measurements will smoothen-out the course of the level. Directly after the plucking attack, the overall level is influenced strongly by the level of the high-frequency partials but these decay rather rapidly. After a short time, a few low-frequency partials dominate: they decay slowly. Therefore, the overall level often decays non-linearly – quickly at first, and then more and more slowly. Because many partials are involved, there is no sharp kink but a rounded off shape of the decay.

♣ More extensively elaborated in: M. Zollner, Signalverarbeitung, Hochschule Regensburg, 2010.

1.6.4 Old strings

For wound strings, the energy share converted into heat depends strongly on the age of the strings. Dirt and remains of skin are deposited in the grooves of the winding; this causes additional damping. Corrosion may also contribute. The mass introduced into the winding has the effect of a detuning; however, the strongest impact is perceivable in the damping of high frequency partials: an old string sounds dull. With electrically amplified guitars it does not help to turn up the treble control, because the decay constant cannot be extended that way.

This figure is reserved for the print version of this book

This figure is reserved for the print version of this book

Fig. 1.51: The decay of an open E_2-string: left for a low-frequency partial, right for a high-frequency partial. "Alte Saite" = old string; "neue Saite" = new string.

In **Fig. 1.51** we see the course of the partial-levels of a decaying E_2-string. For the 2^{nd} partial (164,8 Hz), the differences between old and new string are within the limit of reproducibility: the vibrations decay with practically the same speed. This is very different at high frequencies: the decay duration for the old string is reduced to $1/7^{th}$. The time constant for the decay of the old string is merely 0,1 s; under no circumstance must any measurement of the decay therefore be taken with the FAST setting.

For the E_4-string, no ageing could be found: neither with the fundamental, nor for the higher harmonics. The string had been wiped with a cloth before the measurement, and apparently any residue lets itself readily enough be removed from the solid strings. In contrast, simple wiping does bring only very mild relief for the wound strings. Better results are said to be obtained by ultrasonic baths, or boiling the strings in suitable solvents; we did not carry out any analysis to that end.

Besides corrosion and residue, a further ageing process is to be considered: over time, the frets grind small **transverse grooves** into the strings – action and homogeneity consequently change. Mass and stiffness are not distributed uniformly along the string anymore but depend on the location. For the model of the string, an inhomogeneous transmission line with location-dependent wave-impedance results. Each groove makes for a small mismatch and thus triggers minor reflections. This effect was not analyzed in the scope of this present work.

In conclusion, Chapters 1.5.3 , 7.7.6, and 7.12.2 should be mentioned: for old strings, it is not only the decay process that is different but also the excitation. New strings sound more brilliant because every **bounce** off a fret generates a broadband impulse. In old strings, the deposits act as treble-attenuating buffer.

1.7 Lifetime of strings

How long do guitars strings last? Depends … The collector may be most enthusiastic about that original No-Caster still carrying its original strings that after almost 70 years. The professional may change strings after every gig – or only as a string breaks because the sound of new strings may not be what is liked: "*James, the Paula sounds so piercing.*" " Which one, Milord?" "*The one with the E.C. carved into the headstock ... should be No. 8.*" "Pardon me, Sir, No. 8 is the one with the foot-long whisker pinched in the bridge; the one with E.C. is No. 38. I have just put on fresh strings, and they are not played-in yet".

Strings almost always break at places where they are strongly bent. This is because here the mechanical load is even higher than along the free section of the string. Thus, it would be in the interest of longevity to round off all sharp-edged support points. At a sharp edge, the nickel coating (that in fact provides protection against corrosion) can mutate into an electro-chemical string murderer: if the nickel coating is damaged, humidity and sweat combine with the two metals (steel, nickel) to form a local electric cell. The resulting electrical current leads to subsurface corrosion and, in the end, to string breakage. Fender recommends to add a drop of machine oil or Vaseline to the support points of the string in order to keep humidity and sweat away from the string. That's good advice – that needs to be supplemented with the following: on the Stratocaster, the treble strings experience a sharp bend on an edge on the vibrato block. It is worth the trouble to deburr that edge with a high-grade round file (similar problem areas can be found on other guitars). Why doesn't Fender deburr that edge in the first place? Well … Fender does sell strings, too …

Nicely supported and guided, strings can last for months even when played frequently – but they do sound increasingly dull (Chapters 1.6.4, 7.7.6, and 7.12.2). They will therefore be changed before their final "snap". Whether this happens after a few days or after a few months – that depends to such an extent on the individual approach and taste that it is impossible to give any guide values here. Frequent, heavy handed playing will shorten the lifetime, wiping the strings now and then, and using care products may extend it. In any case, when using the latter, care needs to be taken that such products are compatible with the material of the fretboard!